Measuring the concentration of protein nanoparticles synthesized by desolvation method: comparison of Bradford assay, BCA assay, hydrolysis/UV spectroscopy and gravimetric analysis

Pavel Khramtsov[1,2], Tatyana Kalashnikova[1,2], Maria Bochkova[2], Maria Kropaneva[2], Valeria Timganova[2], Svetlana Zamorina[1,2], Mikhail Rayev[1,2]*

[1]Department of Biology, Perm State University, 614068, 15 Bukirev str., Perm, Russia
[2]Institute of Ecology and Genetics of Microorganisms, Perm Federal Research Center of the Ural Branch of the Russian Academy of Sciences, 614081, 13 Golev str., Perm, Russia
**Corresponding author: e-mail: khramtsovpavel@yandex.ru, phone: +7 (342) 2807794, 614081, 13 Golev str., Perm, Russia*

Abstract

The desolvation technique is one of the most popular methods for preparing protein nanoparticles for medicine, biotechnology, and food applications. We fabricated 11 batches of BSA nanoparticles and 2 batches of gelatin nanoparticles by desolvation method. BSA nanoparticles from 2 batches were cross-linked by heating at +70 °C for 2 h; other nanoparticles were stabilized by glutaraldehyde. We compared several analytical approaches to measuring their concentration: gravimetric analysis, bicinchoninic acid assay, Bradford assay, and alkaline hydrolysis combined with UV spectroscopy. We revealed that the cross-linking degree and method of cross-linking affect both Bradford and BCA assay. Direct measurement of protein concentration in the suspension of purified nanoparticles by dye-binding assays can lead to significant (up to 50-60%) underestimation of nanoparticle concentration. Quantification of non-desolvated protein (indirect method) is affected by the presence of small nanoparticles in supernatants and can be inaccurate when the yield of desolvation is low. The reaction of cross-linker with protein changes UV absorbance of the latter. Therefore pure protein solution is an inappropriate calibrator when applying UV spectroscopy for the determination of nanoparticle concentration. Our recommendation is to determine the concentration of protein nanoparticles by at least two different methods, including gravimetric analysis.

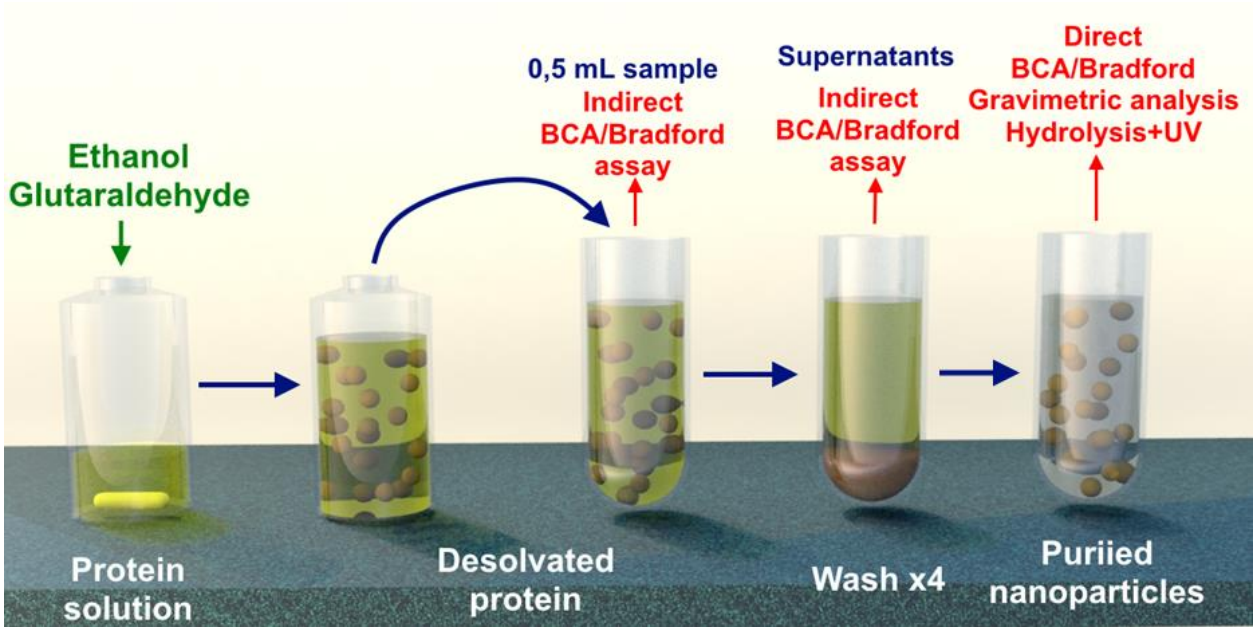

Graphical abstract

Keywords: protein nanoparticles, synthesis, albumin, gelatin, desolvation, yield

Highlights

1. Desolvation procedure and yield of nanoparticles depends on the source of BSA
2. Thermally cross-linked BSA nanoparticles can be used as redox-responsive carriers
3. Cross-linking method and degree both affect results of Bradford and BCA assay
4. Reaction of protein with cross-linking agent changes the UV absorbance of protein
5. We recommend gravimetric analysis for measuring the concentration of nanoparticles

Mention of trade names or commercial products in this publication is solely for the purpose of providing specific information and does not imply recommendation or endorsement by the Perm State University and Institute of Ecology and Genetics of Microorganisms.

1. Introduction

Protein nanoparticles are utilized across a wide and varied range of applications, including therapy, in vitro and in vivo diagnostics, and food chemistry due to their biocompatibility, ability to bind insoluble drugs, diverse chemical structure facilitating functionalization, and other favorable properties. Albumins (bovine serum albumin (BSA), human serum albumin (HSA), ovalbumin), gelatin, casein, whey protein, and plant-derived proteins like zein and gliadin are among the most popular examples of carrier proteins (**Bhushan, 2017**). Cargo-free nanoparticles assembled from functional proteins and polypeptides, for example, viral antigens or enzymes (**Varca, 2014, Wang, 2018, Neelam, 2019, Wang, 2020**), are advantageous tools in vaccine development, biosensing, and biotechnology.

Apart from successful and commercialized nab-technology, there are some other promising techniques for protein nanoparticle synthesis, and desolvation is one of them (**Elzoghby, 2012**). The principle of desolvation is based on the decrease of protein solubility upon the addition of poor solvent (e.g., ethanol, acetone, chloroform) to an aqueous protein solution. Protein molecules change their conformation and aggregate, forming nanoparticles, which are stabilized via chemical, thermal, or radiation-induced cross-linking (**Herrera Estrada, 2015**). After that, unreacted protein, cross-linker, and solvents are removed, and nanoparticles are dispersed in the desired solvent.

The determination of nanoparticle concentration is an essential part of their characterization alongside structural and microscopic investigations. There are several reported methods for quantification of protein nanoparticles:

1. Dye-binding protein assays, as a rule, bicinchoninic acid (BCA) assay, or Bradford assay. These assays can be carried out indirectly by measuring non-desolvated protein (**Yedomon, 2013, Galisteo-González, 2014**) or directly by measuring the concentration of purified nanoparticles (**Chang, 2017**, **Chang, 2018, Deng, 2018, Pustulka, 2020, Habibi, 2020**)
2. Measurement of absorbance at 280 nm (A280) of intact nanoparticles (**Lomis, 2016, Sánchez-Segura, 2018, Tazhbayev, 2019, Arroyo-Maya, 2014**) or non-desolvated protein (**Wang, 2014**)
3. Hydrolytic disruption of nanoparticles with the following determination of A280 in hydrolyzate (**Merodio, 2001, Merodio, 2002**)
4. Gravimetric analysis (**Wacker, 2011, Woods, 2015, Altintas, 2013**)
5. Turbidimetry with the aid of nanoparticle solutions with known concentrations (**Wacker, 2011**)
6. Residual protein in supernatant can be determined by size exclusion chromatography (or HPLC) (**Wacker, 2011; Von Storp, 2012**).

When protein nanoparticles are synthesized for drug delivery purposes, drug loading is performed in the course of desolvation (usually by the dissolution of the molecule of interest in poor solvent). After that, protein nanoparticles are lyophilized as a rule, followed by weighing to determine the encapsulation efficiency of the target molecule. In this case, the direct measurement of nanoparticles' amount is an integral part of nanocarrier preparation. However, when lyophilization is undesirable or suspension of protein nanoparticles should be further processed, nanoparticle concentration in the suspension needs to be determined. Moreover, the assessment of concentration can be a part of in-process control when freeze-drying to be performed (**Wacker, 2011**). In the following applications and situations, determination of protein nanoparticle concentration in suspension is essential:

1. Protein nanoparticles are loaded with therapeutics by incubation. Alongside *in situ* loading, prepared protein nanoparticles can be loaded by incubation with the solution containing the target substance: therapeutic peptides (**Huang, 2017**), antiviral oligonucleotides (**Arnedo, 2004**), prodrugs (**Li, 2015**), radioprotectors (**Kumar, 2016**), anticancer agents (**Karami, 2020**), anti-biofilm agents (**Goswami, 2014**), radiosensitizers (**Huang, 2014**).

2. Protein nanoparticles serve as a carrier for monoclonal antibodies (**Pan, 2019**, **Zong, 2019**), nanobodies (**Altintas, 2013**, **Heukers, 2014**), peptide haptens (**You, 2019**), immunostimulatory oligonucleotides (**Zwiorek, 2007**)

3. Enzyme and albumin nanoparticles are used for electrode modification in biosensors (**Neelam, 2019, Yaman, 2019**, **Liu, 2005**) and signal enhancement in immunoassays (**Lee, 2019**). Gelatin nanoparticles are applied as a support for the immobilization of haptens in solid-phase immunoassays (**Ghoshdastidar, 2020**).

4. Protein nanoparticles prepared by desolvation possess luminescent properties (**Yang, 2016**, **Cai, 2016**). They can be further functionalized and used as labels.

5. Suspensions of protein nanoparticles are also used in the preparation of films for food packaging (**Gilbert, 2017**), carriers of food supplements (**Martins, 2018**), stabilization of Pickering emulsions in food chemistry and pharmaceutics (**Tan, 2014**), manufacturing of 3D porous media for cell growth (**Tan, 2018**), bone regeneration (**Wang, 2016**).

When conducting preliminary studies, we synthesized three BSA nanoparticles batches by desolvation method (see protocol and tables S1, S2, and S3). After desolvation, we determined their concentrations by gravimetric analysis, hydrolysis combined with UV spectroscopy, and Bradford protein assay (direct and indirect). Surprisingly, a substantial discrepancy in results was observed. Indirect and direct Bradford assays, respectively, overestimated and underestimated the nanoparticles' concentration in relation to gravimetric analysis. At the same time, concentration values obtained by gravimetric analysis and hydrolysis/UV did not differ significantly. These findings motivated us to scrutinize various methods for quantification of protein nanoparticles. As far as we know, no comparative investigations on this topic were conducted; however, in several papers dedicated to nanotherapeutics preparation, the concentration of protein nanoparticles was measured by various methods (**Arroyo-Maya, 2014**, **Wacker, 2011**, **Merodio, 2001**). Despite these papers containing short discussion of obtained results, there is still a lack of comprehensive studies.

Against this background, the current work aims to compare different techniques for determining the concentration of protein nanoparticles prepared by the desolvation method. Eleven batches of BSA nanoparticles and two batches of gelatin nanoparticles were synthesized under various experimental conditions. Then nanoparticles were quantified by several methods: gravimetric analysis, direct and indirect dye-binding assays (BCA and Bradford assays), alkaline hydrolysis in combination with UV spectroscopy. We revealed factors that affect results of the mentioned assays and formulated recommendations that will allow the researchers to measure concentrations more accurately. These are summarized in the section 4.

2. Methods

2.1. Materials

Bovine serum albumin was obtained from VWR (USA), lot 0332, Roche (USA), lot 10735078001, and Biosera (France), lot PM-T1725. Gelatin B with bloom number 75 (G6650), BCA assay kit, sodium dodecyl sulfate (SDS), beta-mercaptoethanol, dithiothreitol were obtained from Sigma Aldrich (USA). Glutaraldehyde (50%) was obtained from ITW Reagents (USA), lot A3166, or Sigma Aldrich (USA), lot G7651. Sodium hydroxide, sodium azide, sodium chloride, sodium hydrogen phosphate, sodium dihydrogen phosphate, tris(hydroxymethyl)aminomethane, sodium persulfate, glycerol, and Tween-20 were obtained from ITW Reagents (USA). Ethanol, hydrochloric acid, acetic acid, and methanol were obtained from Reakhim (Russia). Bradford reagent concentrate, 40% acrylamide, and bis-acrylamide solution, tetramethylethylenediamine, Precision Plus Protein™ Dual Color standards, Coomassie Brilliant Blue G-250, Bromphenol Blue were from Bio-Rad (USA). Trypsin was from Samson-Med (Russia). PageRuler protein ladder was obtained from Thermo (USA)

Buffer: phosphate buffer (PB) 0.15 M NaCl, 0.015 M Na_2HPO_4, 0.015 M NaH_2PO_4, and 0.1% NaN_3, pH = 7.25.

Stock solutions of BSA (~50 mg/mL) in deionized water were prepared and stored at +4 °C. Exact concentrations of BSA were measured by UV spectrometry and gravimetric analysis, and shown in Table 2. We determined the BSA concentration using spectrophotometry, considering that the absorbance of a BSA solution's absorbance with a concentration of 1 mg/mL at 280 nm is 0.67.

The following instrumentation was used: peristaltic pump, LKB (Sweden), Synergy H1 plate reader, BioTek (USA), Multiskan Sky UV-Vis Reader, Thermo (USA) and ZetaSizer NanoZS particle analyzer, Malvern (UK), Mini-Protean Tetra Cell electrophoresis device, Bio-Rad (USA) Multipette M4, Eppendorf (Germany) was used for accurate dispensing of viscous BSA and gelatin solutions.

2.2. Synthesis of BSA nanoparticles cross-linked by glutaraldehyde

The pH of stock BSA solutions ranged from 7 to 7.5. We brought the pH of BSA solutions to 9 using 1 M NaOH (approximately 8-10 µL of 1 M NaOH per 1 mL of BSA). The final concentration of NaOH was 8-10 mM. BSA solution (4 mL) was poured into a glass vial and heated to +35 °C. With constant stirring on a magnetic stirrer (1400 rpm), 96% ethanol (4 mL/min) was added (Table 1). The temperature of the solution was monitored using a temperature sensor (Fig. 1).

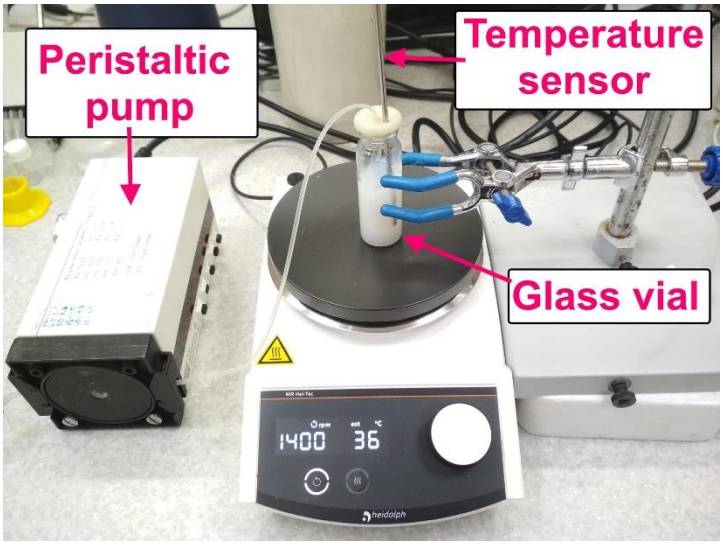

Fig. 1. Experimental setup.

Five minutes after the end of the ethanol addition, 640 µl (or 47 µl for batch NP11) of an 8% aqueous glutaraldehyde solution was added to the suspension. The heating of the suspension was stopped; the cross-linking of nanoparticles was carried out at room temperature for 60 minutes. The color of the suspension gradually changed from white to light brown. A suspension of nanoparticles was divided into ~1 mL aliquots; then, the nanoparticles were washed with water from non-desolvated BSA, ethanol, and glutaraldehyde molecules using four 30-minute-long centrifugation cycles at 20,000 g. The supernatants after each washing cycle were pooled and stored at +4 °C. After each centrifugation pellets were resuspended using ultrasound (probe diameter 3 mm, amplification - 60%, power - 8 W, duration - 20 sec). After the final wash, nanoparticles were resuspended in a certain volume of deionized water and stored at +4 °C.

The concentration of glutaraldehyde was selected based on the method of nanoparticles' zeta-potential measurement (Fig. S1) proposed in the article (**Galisteo-González, 2014**).

Volumes of supernatants and purified nanoparticles were measured by graduated cylinders or by automatic pipettes. Samples of desolvated nanoparticles (500 µL) were collected for protein analysis.

2.3. Synthesis of BSA nanoparticles cross-linked by heating

In general, the synthesis of nanoparticles was performed in the same way as when using glutaraldehyde for cross-linking. After adding ethanol, the suspension was heated to +70 °C and kept for two hours with constant stirring (**Weber, 2000**). The color of the suspension remained white. A suspension of nanoparticles was divided into ~1 mL aliquots, and then the nanoparticles were washed with water by centrifugation at 10,000 g for 30 min. The supernatants after each washing cycle were pooled and stored at +4 °C. After each centrifugation pellets were resuspended using ultrasound (probe diameter - 3 mm, amplification - 60%, power - 8 W, duration - 20 sec). After the final wash, nanoparticles were resuspended in a certain volume of deionized water and stored at +4 °C.

2.4. Synthesis of gelatin nanoparticles

Gelatin was dissolved in water to 26.6 mg/mL (as measured by gravimetric analysis); the pH was adjusted to 9 using 1 M NaOH (approximately 15 µL of 1 M NaOH per 1 mL of gelatin), and the resulting solution was kept at +37 °C. Twelve milliliters of 96% ethanol were added to 4 mL of gelatin solution, and then the mixture was gently shaken and left for 5 min. Formed nanoparticles were cross-linked with 360 µL of 8% glutaraldehyde for 30 min. The concentration of glutaraldehyde was chosen according to Geh et al. (**Geh, 2016**) with four-fold excess. Nanoparticles were divided into ~1 mL aliquots and centrifuged at 8000 g for 10 min. The supernatant was collected for analyses and stored at +4 °C; 1 mL of water was added to the pellets, which were then resuspended by sonication (20 sec, 60% amplification, 3 mm probe). Washing was repeated 4 times. After the final wash, nanoparticles were resuspended in a certain volume of deionized water and stored at +4 °C.

Cross-linking degree of gelatin. Although glutaraldehyde reacts with various amino-acids (**Migneault, 2004**), we measured the cross-linking degree in relation to the number of primary amines of lysine side chains. Gelatin B contains approximately 11 lysine residues per 1000 amino acids (**Hafidz, 2011**). The mean molecular weight of a single amino acid is approx. 110 Da. The molecular weight of gelatin B with a bloom number of 75 is between 20 and 25 kDa. Therefore, each molecule of gelatin B contains 2-2.5 lysine residues. 4 mL of gelatin B solution (26.63 mg/mL) contains approx. 5.3 µM of protein (10.6 µM of lysines). We added 288 µM of

glutaraldehyde and obtained a cross-linking degree of 5400% (54 glutaraldehyde molecules per pair of lysine residues).

Table 1. Synthesis conditions of protein nanoparticles

Batch name	Protein and manufacturer	Cross-linking method	Cross-linking degree (mL of 8% GA per 4 mL of protein)	Ethanol added, mL
NP1	BSA, “VWR”	glutaraldehyde	540%[1] (640)	11,73
NP2	BSA, “VWR”	glutaraldehyde	540% (640)	16
NP3	BSA, “VWR”	glutaraldehyde	540% (640)	16
NP4	BSA, “Roche”	glutaraldehyde	540% (640)	20
NP5	BSA, “Roche”	glutaraldehyde	540% (640)	18
NP6	BSA, “VWR”	Heat treatment, +70 °C	-	16
NP7	BSA, “Biosera”	Heat treatment, +70 °C	-	13,3
NP8	Gelatin B, “Sigma”	glutaraldehyde	5400% (360)	12
NP9	Gelatin B, “Sigma”	glutaraldehyde	5400% (360)	12
NP10	BSA, “Biosera”	glutaraldehyde	540% (640)	13,3
NP11	BSA, “Biosera”	glutaraldehyde	40% (47)	13,3
NP12	BSA, “VWR”	glutaraldehyde	540% (640)	11,73
NP13	BSA, “Biosera”	glutaraldehyde	540% (640)	11,46

[1]Moles of glutaraldehyde/(moles of primary amines/2)×100%

2.5. Bradford protein assay and BCA assay

Both protein assays were performed in 96-well plates. When performing the Bradford assay, 5 µL of the sample and 250 µL of the dye solution were added to the wells. The plate was incubated at +37 °C for 5 min, after which the absorbance of the solution was measured using a microplate spectrophotometer at 595 nm. When performing the BCA assay, 200 µL of a dye solution was added to 25 µL of the sample. The mixture was incubated at +37 °C for 30 min in a thermal shaker, after which the absorbance of the solutions was evaluated at 562 nm. We analyzed aliquots taken immediately after desolvation, aliquots from supernatants, and samples of purified nanoparticles. All samples were diluted 1:1, 1:3, 1:9 and 1:27 in water; samples of concentrated nanoparticles (batches NP9 and NP10) were diluted 1:5, 1:15, 1:45, 1:135. Protein concentrations were calculated using the absorbance values of the lowest dilution that fell within the calibration range.

We used stock BSA solutions (see section 2.1) to prepare calibrators. Since the BSA concentrations obtained by UV spectrometry and gravimetric analysis were different (Table 2), we used both of them when measuring nanoparticle concentration. To construct the calibration curve for gelatin, we used the concentration measured by gravimetric analysis.

Concentration of nanoparticles was calculated by direct method (concentration of purified nanoparticles) and by indirect method:

$$\text{Concentration} = \frac{\text{Initial mass BSA} - (0{,}5 \times \text{Cdes.} + \text{Csup.}1 * \text{Vsup.}1 \; + \; \text{Csup.}2 * \text{Vsup.}2 \; + \; \text{Csup.}3 * \text{Vsup.}3 \; + \; \text{Csup.}4 * \text{Vsup.}4)}{\text{Vnanoparticles}}$$

where Cdes. – concentration of protein after desolvation, Csup.1 – concentration of protein in supernatant after 1st wash, Vsup.1 – volume of supernatant after 1st wash.

A representative example of calculations is given in **the Supporting Information.**

2.6. Acidic and alkaline hydrolysis

The optimization of hydrolysis conditions in preliminary studies was performed as follows. To 1 mL of the sample, 10 M NaOH or HCl was added to a final concentration of 1, 2, or 4 M. The volume of the mixture was adjusted with water to 1666 µL. During BSA hydrolysis, 3.2 µL of 8% glutaraldehyde per 1 mg of BSA was added to each tube. The hydrolysis was carried out in 2 mL microtubes at +37 °C with constant stirring on a rotator mixer (angle 360 degrees, 10 rpm). The hydrolyzate was diluted 1:10 in water, added to quartz cuvettes, and the absorbance was evaluated at 280 nm. For each sample, hydrolysis was carried out in three microtubes.

Alkaline hydrolysis of samples from batches NP1-13. One hundred microliters of BSA nanoparticles' suspension was added to 900 µL of 4.4 M NaOH, nanoparticles from batch NP10 were preliminary diluted 1:10 in water. Gelatin nanoparticles (500 µL) were mixed with 500 µL 8 M NaOH in a final volume of 1 mL; nanoparticles from batch NP9 were preliminary diluted 1:5 in water.

Calibration curves were constructed using untreated or glutaraldehyde-treated stock solutions of BSA (from "Roche") and gelatin. The pH of the BSA solution was adjusted to 9 by 1 M NaOH solution. To the 1 mL of the resulting solution, 8% glutaraldehyde was added in an amount of 160, 11.5, or 0 µL and incubated for 1 hour at room temperature. After that, the volume of all solutions was adjusted with water. A gelatin solution with a 26.6 mg/mL concentration was adjusted to pH 9 using 1 M NaOH solution. To 1 mL of the resulting solution, 90 µL or 0 µL of 8% glutaraldehyde was added and incubated for 1 hour at room temperature. The volumes of solutions were adjusted with water. Two-fold dilutions of the obtained solutions were prepared and used as calibrators; after that, 900 µL of 4.4 M NaOH was added to 100 µL of BSA calibrators, 500 µL of 8 M NaOH was added to 500 µL of gelatin calibrators.

Calibration solutions of BSA and gelatin were prepared in the presence of an excess of glutaraldehyde, and they, therefore, contained unbound glutaraldehyde. To compensate for the 280 nm absorption caused by the presence of free glutaraldehyde, calibration solutions with different concentrations of glutaraldehyde were prepared and treated with 4 M NaOH. Corrected absorbance of BSA/Gelatin calibrators was calculated as follows:

$$A_{280} \text{ of protein} - A_{280} \text{ of X\% GA solution},$$

where X is the concentration of free glutaraldehyde in BSA (or gelatin) calibrator.

We were not able to accurately calculate the number of glutaraldehyde molecules reacted with amino groups of BSA/gelatin; thus, we assumed that all glutaraldehyde presented in calibrators in the free form.

Since BSA concentrations determined by UV spectrometry and gravimetric analysis were different, calibration curves for BSA were constructed concerning both of them. Specifically, the initial BSA "Roche" concentration was 51.60 mg/mL according to UV spectrometry and 56.56 mg/mL according to gravimetric analysis.

The hydrolysis was carried out for 48 hours in 2 mL microtubes at +37 °C with constant mixing on a rotator mixer (angle 360 degrees, 10 rpm). For each sample, hydrolysis was carried out in three microtubes (three replicates). The absorbance of undiluted hydrolyzates was evaluated at 280 nm.

2.7. Gravimetric analysis

Porcelain crucibles were heated at +140 °C to constant weight. Then samples were poured into them in a volume of 100 µL (batches NP9 and NP10) or 1 mL. The water was evaporated at +95 °C, after which the samples were dried to constant weight at +140 °C.

2.8. Fluorescence measurements

Aqueous solutions of gelatin, BSA, and nanoparticles from gelatin B and BSA with a concentration of 1 mg/mL (according to gravimetric analysis) were prepared. One hundred microliters of the obtained solutions were added to the wells of black 96-well plates. Fluorescence was evaluated using a range of excitation wavelengths from 280 to 600 nm (with an interval of 20 nm). The emission spectra were recorded starting from a wavelength of 30 nm longer than the excitation wavelength. When assessing the presence of long-lived fluorescence, the delay before fluorescence measurement was 100 ns. The measurements were made at room temperature.

2.9. Gel electrophoresis

Gel electrophoresis of nanoparticles and supernatants was performed in polyacrylamide gels. Gels were prepared using 0.1 M TRIS-HCl buffer, pH 8.8, and contained 0.1% SDS. TRIS-glycine buffer pH ~8.3 was used as an electrode buffer. Electrophoresis was performed without using a concentrating gel. The gel thickness was 0.75 mm. Nanoparticles were mixed with a sample buffer (10% SDS, 0.1 M EDTA, 50% glycerol, 0.5 M TRIS, 0.1% Bromphenol blue, with or without 50 mM beta-mercaptoethanol) 5:1, 10 µl of the mixture was applied to the gel. In some experiments, the sample buffer contained beta-mercaptoethanol, and the samples were warmed up at +95 °C before being applied to the gel. Samples of supernatants were mixed 1:1 with a 90% solution of glycerol in water. When a smaller amount of glycerol was added, the samples flowed into neighboring wells due to differences in ethanol and water density. The BSA concentration was 1 mg/mL. Electrophoresis was performed at a constant voltage of 200 V. The gels were stained for 60 minutes with Coomassie G-250 and then destained with a fixing solution (20% methanol, 7.5% acetic acid). Destained gels were photographed using a smartphone. Photographs were cropped and presented without any color manipulations.

2.10. Thermogravimetric analysis

A total of 100 µL nanoparticle samples were dried at +95 °C and placed in the TGA furnace. The measurement was carried out under air at a heating rate of 10 K·min−1 from +25 to +1000 °C.

2.11. Size and zeta-potential measurements

Nanoparticle sizes were measured by dynamic light scattering (DLS). Nanoparticles were diluted 1:350 in 750 µL of water. Measurements were performed in 2 mL plastic cuvettes, and 3 technical replicates were performed for each sample. Before measurement, the nanoparticles were thoroughly vortexed. For zeta potential measurements, phosphate buffer was diluted tenfold in water (pH of the diluted buffer was 7.47), then 7 µL of nanoparticles' suspension was added to 700 µl of the diluted buffer. Measurement was performed in 4 mL cuvettes, and 3 technical replicates were performed for each sample.

2.12. UV-VIS spectrometry

The absorbance spectrum of nanoparticles (1 mg/mL) was acquired in the wavelength range from 190 to 1000 nm.

2.13. Stability of Nanoclusters to Proteolytic Digestion

Nanoparticles were diluted to 2 mg/mL with 0.1x PB; then, 200 µl of resulting nanoparticles were transferred into the wells of 96-well plate. Ten microliters of 1 mg/mL trypsin or water (control

samples) were added to each well. The plates were sealed with tape and kept at +37 °C in a thermostat for 24 h without mixing. Three replicates were analyzed for each batch of nanoparticles.

2.14. Data analysis

Acquired data were processed in MS Office Excel, Microsoft (USA). Graphs were prepared in GraphPad Prism 6.01, GraphPad Inc. (USA), and Origin 2020, OriginLab (USA). Statistical analyses were performed in GraphPad Prism 6.01.

The yield of synthesis was defined as a percentage of BSA/Gelatin desolvated to nanoparticles. Yields were separately calculated for initial concentrations of BSA measured by UV absorbance and gravimetric analysis as follows:

$$\text{Yield}, \% = \frac{\text{Concentration of purified nanoparticles} \times \text{volume}}{\text{Initial weight of protein}}$$

3. Results and discussion

To assess the reliability of the obtained results, several batches of protein nanoparticles were synthesized. BSA from three manufacturers was used for the synthesis; besides, gelatin nanoparticles were synthesized using similar technology. Glutaraldehyde was used to cross-link the nanoparticles; the nanoparticles from two more batches were cross-linked by heat treatment. Details of the syntheses of various batches are presented in the table 1. In the study, we did not try to achieve the maximum possible yield in each synthesis. Our goal was to synthesize a sufficiently large number of nanoparticle batches with various formulations to evaluate the influence of different factors on the determination of nanoparticle concentrations by BCA and Bradford protein assays, gravimetric analysis, and hydrolysis in combination with UV spectroscopy.

The final concentration of nanoparticles in the suspension (other things being equal) depends on the desolvating agent's amount (**Weber, 2000**). For BSA from each manufacturer in preliminary experiments, we selected the specific volume of ethanol to achieve the maximum possible turbidity of the suspension, but simultaneously to prevent the formation of aggregates. Note that if the volume of ethanol further increased, then the formation of large particles visible to the naked eye was observed. During the synthesis of nanoparticles, we added an amount of ethanol that did not lead to the formation of such large aggregates but provided high suspension turbidity (high yield). We intentionally decreased the amount of ethanol for several batches (NP1, NP5, NP12, and NP13) to assess the efficiency of different quantification methods when desolvation yield is low.

3.1. The desolvation process differs when BSA from different manufacturers is used

There are few articles devoted to the reproducibility of protein nanoparticle synthesis, especially using reagents from various manufacturers. Recently Jahanban-Esfahlan et al. (**Jahanban-Esfahlan, 2016**) have discussed some discrepancies in the results obtained by different authors. Specifically, they found out that desolvation of protein under buffered conditions and in the presence of sodium chloride leads to the formation of large protein aggregates, even though numerous papers describe successful desolvation of BSA or HSA in the presence of buffer salts (e.g., **Galisteo-González, 2014**; **Tarhini, 2018**, **Woods, 2015**). At the same time, Langer et al. (**Langer, 2003**) failed to synthesize HSA nanoparticles in the presence of buffer salts but synthesized them using 10 mM NaCl as background electrolyte. In our work, we were facing the same problem: all attempts to synthesize nanoparticles in the presence of salts resulted in forming a large piece of protein similar to the one described by (**Jahanban-Esfahlan, 2016**). For this reason, we dissolved BSA and gelatin in deionized water with the addition of a small amount of sodium hydroxide. Interestingly, we could not reproduce the synthesis of albumin nanoparticles

with EDC cross-linking, which was reported by (**Jahanban-Esfahlan, 2016**). This once again highlights the need to compare reagents from different manufacturers. Previously, Langer et al. (**Langer, 2008**) prepared nanoparticles by desolvation technique using different batches of native and recombinant HSA and showed that the presence of molecular aggregates, as well as di - and trimers of HSA, can affect the size, polydispersity, and yield of nanoparticle synthesis. However, there was no clear relationship between the content of high-molecular forms and the result of nanoparticle synthesis. The authors of the mentioned work suggested that low-molecular impurities can also influence the synthesis result. The presence of low-molecular-weight gelatin fractions led to the formation of aggregates during the synthesis of gelatin nanoparticles (**Coester, 2000**). Type of protein (native, recombinant) affects the size of nanoparticles, besides lot-to-lot variability also takes place (**Luebbert, 2017**).

Different volumes of ethanol were required to initiate desolvation of BSA from various manufacturers: “VWR” - 2.83 mL (mL of ethanol per mL of BSA), “Roche” - 4 mL, “Biosera” - 2.66 mL. Moreover, in the case of BSA from "VWR", this value also varied from day to day (up to 3.16 mL). Microparticles visible were formed during desolvation, and their amount depended on the added volume of ethanol. The most intense formation of microparticles was observed during the preparation of batch NP4. Interestingly, there were no microparticles in the solutions of purified nanoparticles, most likely due to multiple ultrasound treatments during washing. Polydispersity indices were lower than 0.2 for all batches (Table 3). In the course of almost all syntheses, desolvated protein sedimented on the walls of the vial and the magnet (Fig. S2). We washed and collected sedimented protein to minimize its losses.

The yield of nanoparticles synthesis also depends on the protein manufacturer. Yields were noticeably lower (Table S4) for nanoparticles prepared from BSA provided by Roche (NP5 and NP6), despite the largest volumes of ethanol being added (4,5 and 5 mL of ethanol per 1 mL of BSA “Roche”). We should note that the concentration of BSA “Roche” in stock solution was slightly lower (approx. 5% according to gravimetric analysis; no difference was detected by UV absorbance) than that of BSA from VWR and Biosera (Table 2). However, we suppose that such a low difference in initial concentrations cannot explain significant differences in the desolvation process. Additionally, we analyzed results provided by other researchers (Table S5**)** and also revealed considerable differences in desolvation yields**.** Production yields between 39 and 66% in similar synthesis conditions (no salts, slightly alkaline pH) were reported (Table S5, #1-4). Oppositely, in current work, yields were from 54 to 91% (as measured by gravimetric analysis). Note that yield can vary significantly even when the same research group performs desolvation under identical conditions (Table S5, #7 and #8).

The presence of high- and low molecular weight contaminants can lead to variations in the desolvation process. We analyzed BSA from three manufacturers by SDS-PAGE in 6% and 12% gels (Fig. 2). Some samples were heated and contained beta-mercaptoethanol. No significant differences were detected except for BSA from “Biosera” which contained an additional protein band with a molecular mass slightly lower than that of BSA. Dimers of BSA and other proteins with molecular weights between 100 and 200 kDa were in all samples in some amount.

We suppose that differences in nanoparticle preparation stem from the presence of fatty acids in BSA preparations. Recently, the effect of fatty acids on the both size and yield of BSA nanoparticles was confirmed in a study by Luebbert et al. (**Luebbert, 2017**).

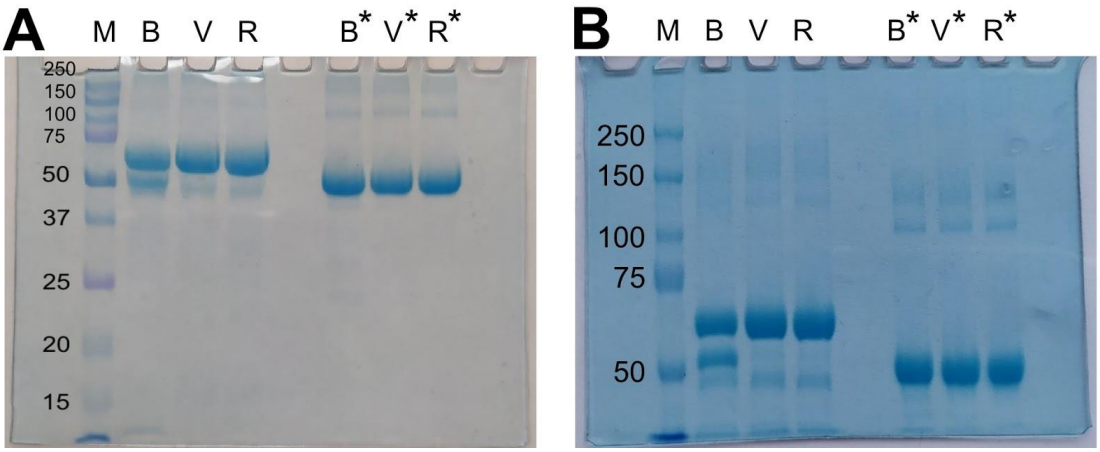

Fig. 2. SDS-PAGE of BSA (1 mg/mL) from three manufacturers in 12% (A) and 6% (B) polyacrylamide gel in reducing (*) conditions (heating at +95 °C for 5 min and addition of beta-mercaptoethanol) or non-reducing conditions. BSA manufacturers: B - "Biosera", V - "VWR", R - "Roche". M - protein markers.

3.2. Two methods for measuring the concentration of BSA in solution showed different results

Stock solutions of BSA from each manufacturer with a concentration of about 50 mg/mL were prepared. The exact concentration of BSA was estimated spectrophotometrically by absorption at 280 nm and gravimetrically by drying 1 mL of BSA solution at + 140 °C. Unexpectedly, the BSA concentrations measured by the gravimetric analysis were more than 10% higher (Table 2). Similar differences were previously reported by Pace et al. (**table 1 in Pace, 1995**). They found that the coefficients of molar extinction of proteins measured by gravimetric analysis are lower than those obtained using the Edelhoch method. The reasons why gravimetric analysis overestimates protein concentration compared to UV-Vis spectrometry was previously discussed by Pace et al. and Anders et al. (**Pace, 1995**; **Anders, 2003**) and residual moisture in BSA powder is one of them. Stamey et al. showed that gravimetric analysis overestimated the concentration of prostate-specific antigen by approximately 20% compared to amino acid analysis and attributed the observed difference to residual moisture in protein preparation (**Stamey, 1995**). We assumed that all the bound water was not removed during the gravimetric analysis. To confirm this assumption, we evaluated the concentration of BSA "Biosera" by TGA. According to TGA, the BSA concentration was lower than the concentration measured by gravimetric analysis but still higher than the concentration measured by UV spectrometry (Table 2). We calculated the yield of nanoparticle synthesis and the results of BCA and Bradford analyses concerning BSA concentrations obtained by both gravimetric and spectrophotometric methods.

Table 2. Concentration of BSA (mg/mL) in stock solutions determined by various methods.

BSA manufacturer	Absorbance at 280 nm	Gravimetric analysis	TGA
VWR	51.8	59.03	ND[1]
Roche	51.6	56.27	ND
Biosera	51.5	58.57	55.4

[1] - not done

3.3. Characterization of synthesized nanoparticles

We fabricated 11 batches of BSA nanoparticles (NP1-7 and NP10-13) and 2 batches of gelatin nanoparticles (NP8 and NP9) by desolvation method. Nanoparticles from 2 batches (NP6 and NP7) were cross-linked by heating at +70 °C for 2 h; other nanoparticles were stabilized by glutaraldehyde. We changed the cross-linking degree from excessive to moderate (40%, 0,4 aldehyde groups per 1 amino group) for batch NP11. Batches NP9 and NP10 with an increased concentration of nanoparticles were used in TGA assay. We prepared gelatin nanoparticles by a modified one-step desolvation technique, which allows using low-molecular-weight gelatin as a source of nanoparticles. A thorough description of this method will be presented in future papers. Herein we just used the developed method to fabricate two batches of gelatin nanoparticles to reveal whether our findings regarding methods for measuring concentration are applicable to nanoparticles prepared from protein other than BSA. Characteristics of nanoparticles are summarized in Table 3 and in Fig. S3, S4

Table 3. Characteristics of synthesized protein nanoparticles

Batch	Volume, mL	z-average diameter, nm (mean±SD)	PdI (mean±SD)[1]	Zeta potential, mV (mean±SD)
NP1	13,9	146,3±0.0[2]	0,096±0.008	-33,2±0,5
NP2	17,5	157,3±1.6	0,088±0.003	-37,6±1,2
NP3	16	153,8±1.1	0,076±0.007	-36,4±0,6
NP4	15,5	139,4±2.3	0,127±0.016	-36,3±0,3
NP5	15	143,1±1.7	0,151±0.003	-37,1±1,9
NP6	13,5	166,8±1.1	0,047±0.013	-21,9±0,6
NP7	12,4	208,0±25.4	0,086±0.039	-20,0±1,2
NP8	12,4	491,3±18.5	0,149±0.049	-11,6±0,5
NP9	2,116	495,7±35.3	0,130±0.074	-11,8±0,2
NP10	1,412	175,1±4.3	0,033±0.020	-34,1±0,4
NP11	14	172,8±1.3	0,046±0.025	-22,1±0,6
NP12	12,2	140,5±1.2	0,166±0.025	-32,3±1,6
NP13	12,2	163,3±2.1	0,109±0.023	-32,3±0,6

[1] - polydispersity index

[2] - n=3

The size of BSA nanoparticles was determined by DLS and was in the range between 140 and 200 nm (Table 3). Gelatin nanoparticles have hydrodynamic diameters (z-average diameter) of 490 nm. All the nanoparticle preparations were relatively monodisperse (PdI from 0.03 to 0.17). Zeta potential of BSA nanoparticles NP6, NP7, and NP11 was between -20 and -22 mV, whereas nanoparticles from other batches had zeta-potential lower than -32 mV. Nanoparticles NP11 had a lower cross-linking degree (40%), whereas NP6-7 were cross-linked by heating. We associate a higher zeta potential with a larger number of amino groups on the surface of nanoparticles. In the synthesis of other nanoparticle batches, an excess of glutaraldehyde was used, which led to a decrease in the zeta potential (**Galisteo-González, 2014**). Zeta potential of gelatin nanoparticles was approximately -11 mV, which is because of a lower percentage of polar acidic and basic amino acids (aspartic acid, glutamic acid, lysine, arginine, histidine) in gelatin B in

comparison with BSA (10,9% vs. 44,7%) (**Hafidz, 2011**, **Heine, 1991**). Despite zeta potential being lower than the widely accepted stability threshold of ±25-30 mV, all nanoparticles were stable in water. Heat-stabilized nanoparticles quickly aggregated in a neutral phosphate buffer containing 0.15 M of NaCl. The stability of gelatin nanoparticles in the buffer was not assessed. Note that we measured zeta potential in the phosphate buffer diluted tenfold with water (pH 7.47).

Nanoparticles were kept at +4 °C and remained stable for at least 2 months, except for NP11, which dissolved after circa 1.5 months of storage (Fig. 3). Batch NP11 was synthesized according to Weber et al. (**Weber, 2000**) to assess the influence of the cross-linking degree on the determination of nanoparticle concentration. Authors of the mentioned paper found out that a cross-linking degree of 40% and higher provides stable HSA nanoparticles, while a lower degree produces unstable nanoparticles that are partially redissolved. Note that a dramatic decrease of turbidity was not accompanied by a change of hydrodynamic diameter of nanoparticles (z-average diameter was 175.7±1.3 nm, PdI was 0.062±0.017). The structure of NP11 after 1.5 months of storage was also evaluated by SDS-PAGE in both reducing and non-reducing conditions (Fig. S4). Large protein smears were on the top of the gel, and no bands corresponding to BSA monomers or oligomers were revealed. The addition of a reducing agent increased the number of protein aggregates entering the gel. In total, these results indicate that a significant percentage of NP11 nanoparticles disintegrated into smaller pieces (probably tens of nanometers); however, nanoparticles of initial diameter were still present as indicated by the DLS study. These large nanoparticles produced high enough light scattering in DLS experiments, and thus no change of mean hydrodynamic diameter was detected. The light scattering value of small pieces of nanoparticles is negligible and does not contribute to the overall scattering of the sample.

In earlier works (**Weber, 2000**, **Anhorn, 2008**), the long-term storage stability of HSA nanoparticles with a cross-linking degree of 40% has not been reported. Weber et al. (**Weber, 2000**) examined the properties of such nanoparticles after two weeks of storage. We cannot unambiguously explain the degradation mechanism of NP11; however, we assume that not only glutaraldehyde stabilized these nanoparticles, but other types of covalent and non-covalent bonds can be formed. For example, disulfide bonds form between BSA molecules in 50% ethanol solution even at room temperature, i.e., ethanol provides cross-linking by itself (**Lambrecht, 2016**). The reshuffling of disulfide bonds occurring upon storage (**Rombouts, 2015**) can result in the disintegration of nanoparticles into smaller pieces. Further degradation of these pieces into BSA mono- and oligomers does not occur (at least in the course of 1-2 months at +4 °C) because they are stabilized by glutaraldehyde. Note that we confirmed partial cross-linking of NP11 by several indirect methods: the color of suspension, fluorescence, protease digestion (see below).

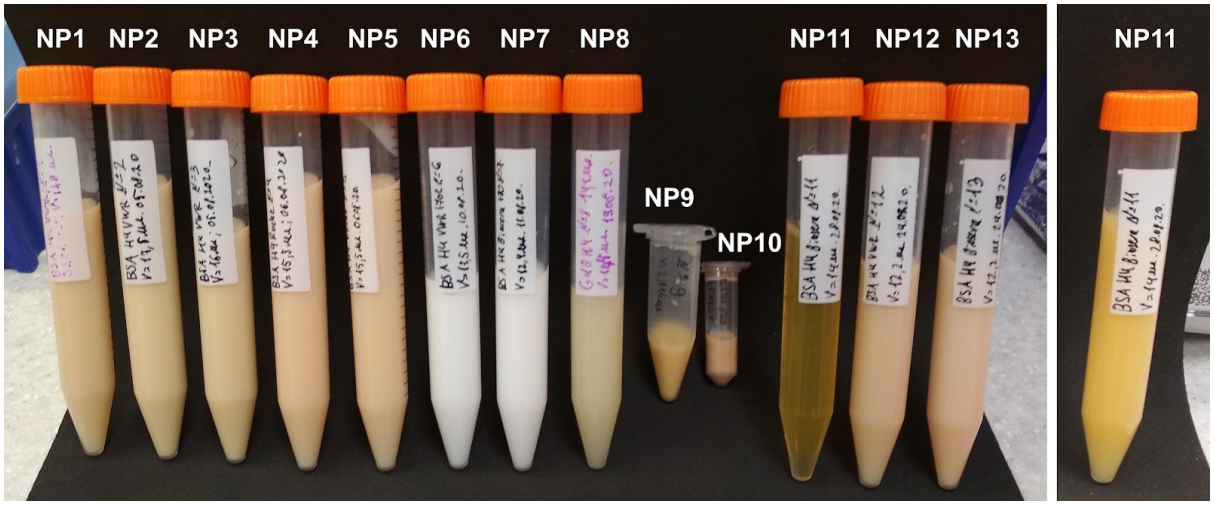

Fig. 3. Suspensions of BSA and gelatin nanoparticles after 1 week (NP12 and NP13) or 1.5-2 months (NP1-11) of storage (left). Suspension of NP11 after 1 week of storage (right).

Batches NP6 and NP7 are heat-stabilized nanoparticles that were cross-linked by heating at +70 °C for 2 h (**Weber, 2000**) instead of glutaraldehyde. These two batches have white color, whereas other nanoparticle suspensions vary from light-brown to yellow. The color of both BSA molecules and BSA nanoparticles and its intensity depended on the cross-linking degree (Fig. 3 and Fig. 11D). Suspension of NP11 has a yellow color, NP1-7, NP10, NP12, and NP13 are light-brown. Surprisingly, Yu et al. (**Yu, 2014**) reported that glutaraldehyde-treated nanoparticles had white color while heat-stabilized ones were yellow. We cannot explain this contradiction. In our experiments, glutaraldehyde addition produced yellowish or light brown particles.

Weber et al. (**Weber, 2000**) supposed that heating at +70 °C leads to the stabilization of BSA aggregates through the formation of intermolecular amide bonds. Authors referred to the paper by Esposito et al. (**Esposito, 1996**), which in turn, cited work by Yannas and Tobolsky (**Yannas and Tobolsky, 1967**). The latter describes the formation of amide bonds in proteins upon heating; however, authors concluded that primary amine/carboxyl condensation requires excessive dehydration, low pressure, and prolonged exposition to high temperature (**Yannas and Tobolsky, 1967**). Therefore the formation of multiple amide bonds during short and mild heat treatment of BSA in the presence of water excess is highly unlikely.

We suppose that disulfide bonds play a primary role in the stabilization of thermally cross-linked BSA nanoparticles. Disulfide bonds form between BSA molecules in 50% ethanol solution even at room temperature, i.e., ethanol provides cross-linking by itself (**Lambrecht, 2016**). Disulfide and non-covalent (e.g., hydrophobic) bonds (**Mine, 1995**) were responsible for the aggregation of ovalbumin (**Croguennec, 2007**), BSA (**Havea, 2001**), IgG (**Futami, 2017**), and formation of OVA nanoparticles upon heating (**Croguennec, 2007**). Li et al. synthesized BSA nanoparticles using heat-driven aggregation and studied alteration of functional groups during heating (**Li, 2016a**). They found that a decrease of thiol, amine, and carboxyl groups occurred during heating and inferred that the formation of disulfide and amide bonds takes place. Nevertheless, we should emphasize that the decrease of free amine and carboxyl groups was rather small, approximately 4-6%. At the same time, the percentage of free thiol groups dropped by approximately 60%, suggesting the formation of disulfide bonds was much more intense. We studied NP6 and NP7 by SDS-PAGE in both reducing and non-reducing conditions. Suspensions of nanoparticles were treated in three different ways before SDS-PAGE. Two samples were heated at +95 °C for 5 min with or without beta-mercaptoethanol; the third sample was kept intact. Samples without beta-mercaptoethanol did enter the gel, whereas the addition of reducing agent led to the appearance of the band at circa 70 kDa, which corresponds to BSA monomer (Fig. 4B, C). Moreover, some amount of high-molecular-weight aggregates entered the gel when beta-mercaptoethanol was presented in the sample. Partial degradation of heat-treated BSA nanoparticles shows that disulfide bonds play a significant role in their stabilization. On the other hand, beta-mercaptoethanol by itself did not provide complete dissolution of heat-treated BSA nanoparticles. We kept NP6 and NP7 for several days in the presence of excess reducing reagents (beta-mercaptoethanol and dithiothreitol), but both suspensions remained turbid (**data not shown**). For comparison, redox-sensitive nanoparticles cross-linked with bifunctional agents are dissolved within tens of minutes in the presence of a reducing agent (**Xu, 2012**). Gulzar et al. showed that heating of protein leads to the formation of intermolecular bonds other than disulfide (**Gulzar, 2011**). The variety of possible covalent bonds between protein molecules caused by different physical and chemical factors was previously discussed by Gerrard (**Gerrard, 2002**).

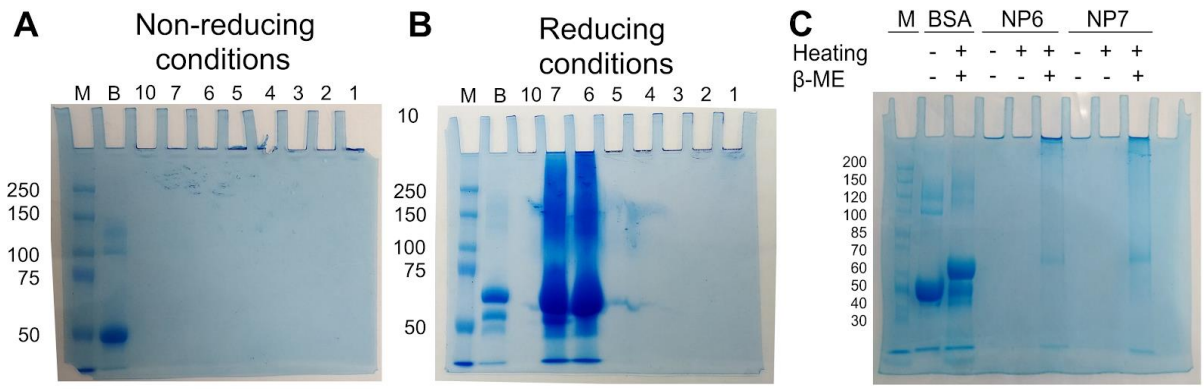

Fig. 4. SDS-PAGE of NP1-NP7 and NP10 in non-reducing (A) and reducing (B) conditions (undiluted nanoparticles). C - SDS-PAGE of NP6 and NP7 in reducing and non-reducing conditions (nanoparticle concentration - 1 mg/mL as determined by gravimetric analysis). Legend: Heating temperature - +95 °C. β-ME - beta-mercaptoethanol. B - BSA. M - protein markers. Concentration of BSA - 1 mg/mL. Polyacrylamide concentration is 6%, voltage - 200 mV.

In our opinion, temperature-stabilized BSA nanoparticles have some potential to be used as redox-responsive carriers for intracellular and intratumoral delivery (**Guo, 2018**). Typically, redox-responsive protein nanoparticles require protein pre-treatment with reducing agents such as glutathione (**Wang, 2013**) or the application of peculiar cross-linkers (**Xu, 2012**). The advantage of heat-stabilization is that it avoids pre-treatment of BSA with a reducing agent (e.g., dithiothreitol) and the need to remove it (**Hassanin and Elzoghby**, **2020**).

Nanoparticles stabilized with excess glutaraldehyde did not enter the gel regardless of the presence of a reducing agent (Fig. 4A,B; Fig. S4, S5), as previously reported (**Pustulka, 2020**). In the paper by Tarhini et al., the BSA band was detected in PAGE of BSA nanoparticles (**Tarhini, 2018**). The authors of this work compared the properties of cross-linked and non-cross-linked nanoparticles and did not clarify what kind of BSA nanoparticles was analyzed. Dissociation of non-cross-linked ones could lead to the appearance of a BSA band. Gelatin nanoparticles were not analyzed by SDS-PAGE.

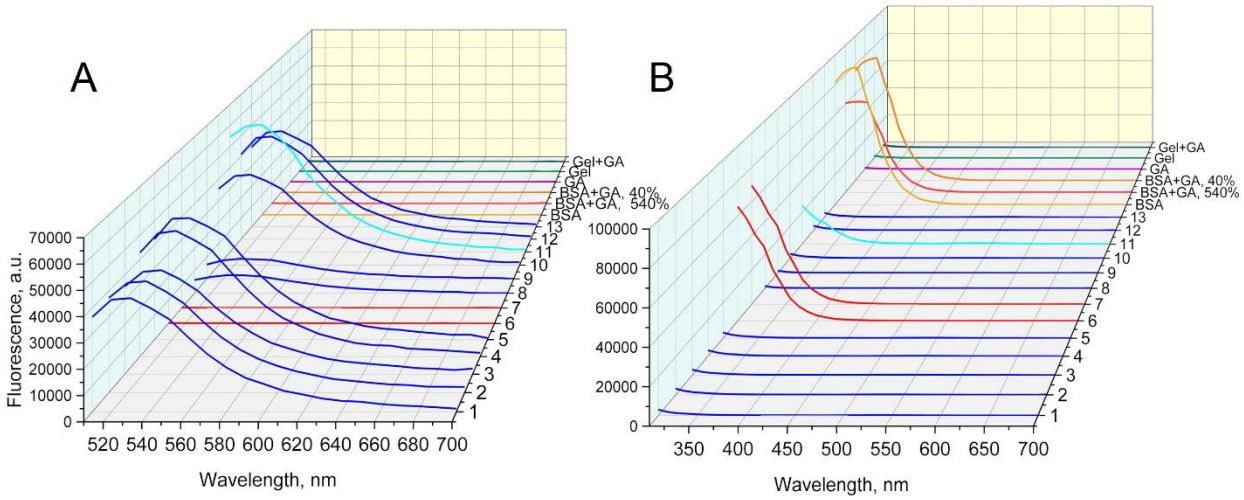

Fig. 5. Fluorescence emission spectra of BSA, gelatin, glutaraldehyde and BSA/gelatin nanoparticles. Excitation wavelength: A – 480 nm; B – 280 nm. Concentration of proteins and nanoparticles is 1 mg/mL. GA – glutaraldehyde.

Fluorescence measurements were used to characterize protein nanoparticles. Two tryptophan residues in the BSA molecule render it fluorescent in the UV region (λ_{ex}=280 nm).

Glutaraldehyde cross-linking suppresses tryptophan fluorescence due to the interaction of aldehyde with lysine or arginine located nearby tryptophan residues (**Liu, 2018**). These reactions lead to a change of tryptophan microenvironment and consequently decrease and blue-shift intrinsic fluorescence of BSA. Similarly, a decrease of tryptophan fluorescence intensity upon cross-linking was shown for α-lactalbumin in solution (**Arroyo-Maya, 2014**). Fluorescence intensity of BSA nanoparticles excited at 280 nm correlated with the concentration of glutaraldehyde (Fig. 5B). The drop of tryptophan fluorescence was observed in BSA nanoparticles cross-linked with an excess of glutaraldehyde, but not in heat-stabilized nanoparticles (NP6 and NP7). Fluorescence intensity of partially cross-linked nanoparticles (NP11) was substantially higher than that of completely cross-linked nanoparticles. A similar fluorescence pattern was observed for BSA molecules treated with glutaraldehyde: an excess of aldehyde decreased fluorescence. Note that fluorescence of BSA nanoparticles was blue-shifted compared to BSA in accordance with previous reports (**Peña and Domínguez, 2010**, **Asghar, 2014**). Thus, UV fluorescence can be used for the measurement of the cross-linking degree. Gelatin B molecules lack tryptophan residues, and no UV fluorescence was detected.

Gelatin and BSA nanoparticles exhibited a wide green fluorescence emission peak with a maximum at 520-530 nm when illuminated at 480 nm (Fig. 5A). The emission intensity of gelatin nanoparticles was approximately 4-6-fold lower. Thermally cross-linked BSA nanoparticles had no fluorescence at this exciting wavelength. Green fluorescence of glutaraldehyde-treated BSA and gelatin nanoparticles corresponds well with the previous results (**Cai, 2016**, **Ma, 2016**). Fluorescence is attributed to the π-π* transition of C=C bond of glutaraldehyde molecules and n-π* transition of C=N bond of Shiff base (**Wei, 2007**). Notably, glutaraldehyde-treated BSA and gelatin had no emission indicating the role of protein aggregation and cross-linking in the emergence of green fluorescence.

From literature, it is known that cross-linking intensity and amino acid composition of protein affect the stability of nanoparticles prepared from this protein to protease digestion (**Elzoghby, 2013**). Gelatin contains a low percentage (1,1% for gelatin B) of lysine residues (**Hafidz, 2011**), whereas BSA contains 11,4% of lysine residues (**Heine, 1991**) thus cross-linking density significantly higher in BSA nanoparticles (when glutaraldehyde is added in excess). We incubated 1 mg/mL suspensions of BSA (NP3, NP4, NP6, NP11) and gelatin nanoparticles (NP8) with 50 μg/mL of trypsin (**Langer, 2008**) at pH 7 for 18 h. The turbidity of all tested batches rapidly decreased except for NP3 and NP4 (Fig. 6), which also is in agreement with the previous reports (**Kommareddy and Amiji, 2008**, **Langer, 2008**). In control samples (without trypsin), absorbance at 600 nm remained unchanged (**data not shown**).

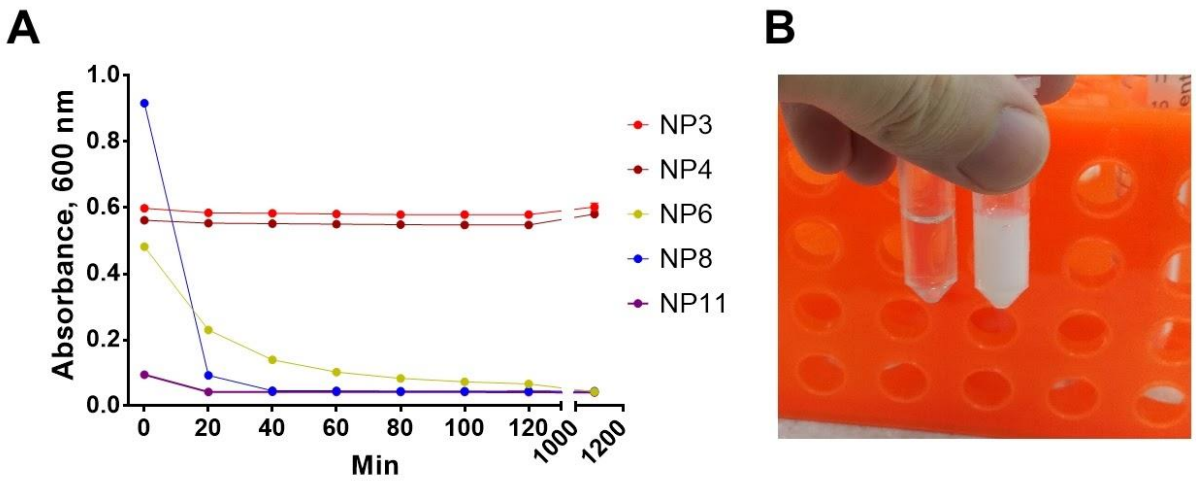

Fig. 6. A - Proteolytic degradation of BSA and gelatin nanoparticles (n=3). Concentration of proteins and nanoparticles is 1 mg/mL. Concentration of trypsin is 50 μg/mL. B - NP6 (5 mg/mL) after 60 min incubation with (left) or without (right) trypsin.

We can conclude that method and degree of cross-linking significantly affect their susceptibility to degradation. In the next sections, we will demonstrate that structure of nanoparticles influence the results of BCA and Bradford protein assays.

3.4. Comparison of methods for assessing the concentration of nanoparticles

In the section 1, we listed the most popular methods for protein nanoparticle quantification. The following methods were chosen for comparative studies: BCA protein assay, Bradford protein assay, gravimetric analysis, and hydrolysis in combination with UV spectroscopy. We calculated the concentration of nanoparticles in final suspension for each batch and determined the yield of synthesis (fraction of the original amount of protein converted to nanoparticles).

Note that we made calculations considering that concentrations of BSA in stock solutions measured by UV spectroscopy (absorbance at 280 nm) and gravimetric analysis were different. BSA concentration in stock solutions affects the yield value, besides stock solutions of BSA were used to prepare calibrators for BCA assay, Bradford assay, and hydrolysis experiments. We determined concentrations and yields in relation to concentrations of BSA determined by both methods separately. Gelatin concentration in the stock solution was determined only by gravimetric analysis.

Concentrations and yields of synthesis for batches of BSA and gelatin nanoparticles are given in Table 4 and Table S4, respectively. To facilitate the comparison of methods, we made a Table 5 containing data on the differences in the concentrations of nanoparticles measured by different methods. This table shows the difference between the concentration of nanoparticles measured using a specific method in relation to the concentration determined using gravimetric analysis.

The concentration of nanoparticles was measured by BCA and Bradford assay in two ways: directly and indirectly (Fig. 7). The direct method is the detection of protein content in the suspensions of purified nanoparticles. To do this, we mixed nanoparticles with BCA or Bradford reagents and measured absorbances at corresponding wavelengths. The indirect method involves determining the concentration of non-desolvated protein in the supernatants obtained by washing the nanoparticles. The concentration of nanoparticles was calculated by subtracting the total protein amount in the supernatants from the initial protein amount. The protein amount in stock solutions was determined using gravimetry and UV spectroscopy, as mentioned above.

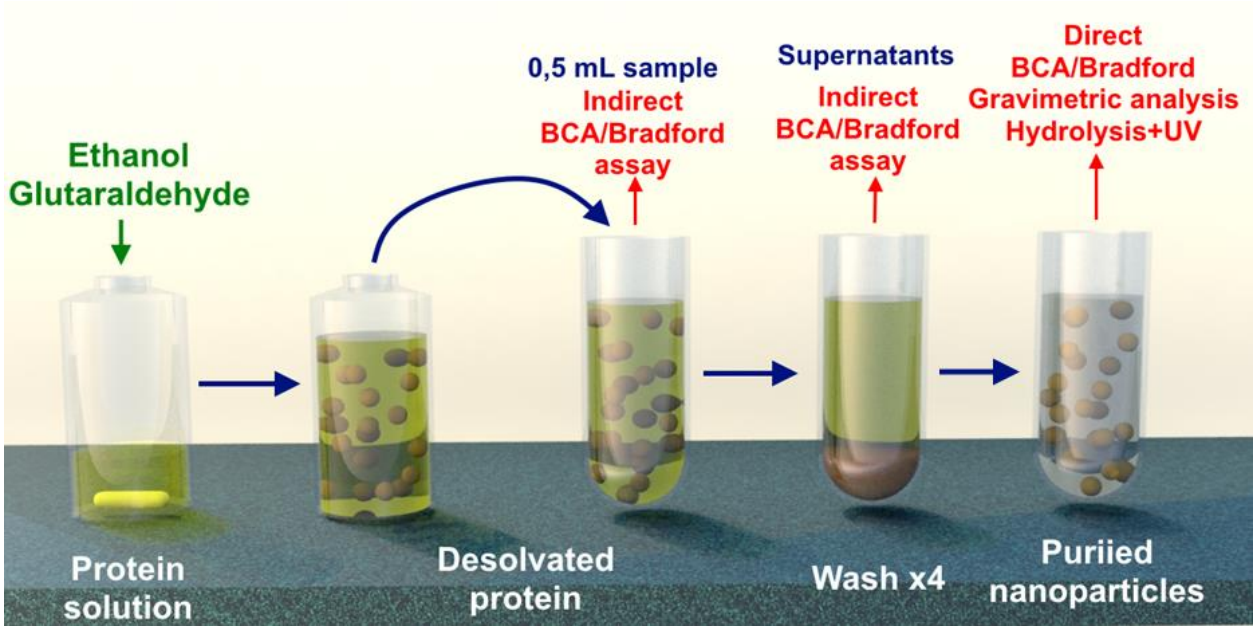

Fig. 7. Design of comparative study

Generally, concentrations of BSA nanoparticles NP6, NP7, and NP11 determined by all tested methods differed insignificantly in contrast to other batches of BSA nanoparticles (Table 5). Batches NP6, NP7, and NP11 were stabilized by heating or a low concentration of glutaraldehyde. For batches NP1-5, NP10, and NP12-13 concentration was significantly lower when measured directly by BCA or Bradford assay. A more complex situation was observed for gelatin nanoparticles (NP8 and NP9). Analysis and a possible explanation of differences are given in the following sections. We discussed the results obtained by each method and revealed possible sources of incorrect results.

Table 4. Concentrations of nanoparticles determined by different methods (in mg/mL)

Batch	Gravimetric analysis	In relation to BSA concentration measured by UV spectroscopy				In relation to BSA concentration measured by gravimetric analysis				Hydrolysis, In relation to BSA concentration measured by UV spectroscopy	Hydrolysis, In relation to BSA concentration measured by gravimetric analysis
		Bradford assay		BCA assay		Bradford assay		BCA assay			
		Indirect	Direct	Indirect	Direct	Indirect	Direct	Indirect	Direct		
NP1	11,36	11,29	4,55	11,13	4,63	12,86	5,19	12,69	5,28	8,39	9,53
NP2	12,36	11,29	3,78	11,16	5,1	12,87	4,31	12,71	5,81	8,89	10,09
NP3	13,5	12,21	4,05	12,12	4,87	13,94	4,7	13,86	5,57	9,74	11,06
NP4	9,86	10,65	3,26	10,28	4,81	11,61	3,55	11,22	5,24	7,16	8,13
NP5	8,2	10,57	2,58	9,88	3,53	11,2	2,82	10,78	3,84	5,88	6,67
NP6	13,3	12,5	10,12	12,27	12,96	14,26	11,53	13,99	14,77	12,37	14,02
NP7	11,9	11,09	10,81	11,75	12,37	12,61	12,3	13,34	14,07	11,22	12,71
NP8	3,5	ND[1]	ND	ND	ND	ND	ND	3,27	4,42	ND	2,44
NP9	18,6	ND	ND	ND	ND	ND	ND	15,49	26,67	ND	14,11
NP10	123	125,29	34,42	127,2	42,37	142,46	60,28	147,38	42,32	86,42	98,07

NP11	12,76	12,85	10,29	12,1	11,82	14,61	11,7	14,4	13,43	12,27	13,93
NP12	11,63	12,6	3,67	13,02	3,81	14,34	4,28	14,77	4,44	ND	ND
NP13	10,87	10,8	4,48	11,21	3,86	12,28	5,12	12,68	4,42	ND	ND

[1] - not done

Table 5. Difference of nanoparticle concentrations determined by gravimetric analysis and by various methods (in %). Color scheme reflects the nature of the differences: red - underestimation, green – overestimation

Batch	Grav. anal.	In relation to BSA concentration measured by UV spectroscopy				In relation to BSA concentration measured by gravimetric analysis				Hydrolysis, In relation to BSA concentration measured by UV spectroscopy	Hydrolysis, In relation to BSA concentration measured by gravimetric analysis
		Bradford assay		BCA assay		Bradford assay		BCA assay			
		Indirect	Direct	Indirect	Direct	Indirect	Direct	Indirect	Direct		
NP1	0,00	-0,62	-59,95	-2,02	-59,24	13,20	-54,31	11,71	-53,52	-26,10	-16,13
NP2	0,00	-8,66	-69,42	-9,71	-58,74	4,13	-65,13	2,83	-52,99	-28,08	-18,37
NP3	0,00	-9,56	-70,00	-10,22	-63,93	3,26	-65,19	2,67	-58,74	-27,82	-18,09
NP4	0,00	8,01	-66,94	4,26	-51,22	17,75	-64,00	13,79	-46,86	-27,35	-17,55
NP5	0,00	28,90	-68,54	20,49	-56,95	36,59	-65,61	31,46	-53,17	-28,34	-18,67
NP6	0,00	-6,02	-23,91	-7,74	-2,56	7,22	-13,31	5,19	11,05	-6,99	5,41
NP7	0,00	-6,81	-9,16	-1,26	3,95	5,97	3,36	12,10	18,23	-5,71	6,81
NP8	0,00	ND[1]	ND	ND	ND	ND	ND	-6,57	26,29	ND	-30,29
NP9	0,00	ND	ND	ND	ND	ND	ND	-16,72	43,39	ND	-24,14
NP10	0,00	1,86	-72,02	3,41	-65,55	15,82	-50,99	19,82	-65,59	-29,74	-20,27
NP11	0,00	0,71	-19,36	-5,17	-7,37	14,50	-8,31	12,85	5,25	-3,84	9,17
NP12	0,00	8,34	-68,44	11,95	-67,24	23,30	-63,20	27,00	-61,82	ND	ND
NP13	0,00	-0,64	-58,79	3,13	-64,49	12,97	-52,90	16,65	-59,34	ND	ND

[1] - not done

3.5. BCA and Bradford protein assays: direct method

Dye-based protein assays are extensively used for protein and protein nanoparticle quantification. Bradford assay is based on the binding of Coomassie Brilliant Blue G-250 dye to arginine, histidine, phenylalanine, tryptophan, and tyrosine residues and hydrophobic interactions of dye and protein. The dye changes the absorbance when bound to a protein, the concentration of which can be calculated by measuring absorbance at 595 nm (**Noble and Bailey, 2009**). Bicinchoninic assay (BCA) relies on the reduction of Cu^{2+} to Cu^{1+} by cysteine, cystine, tryptophan, tyrosine, and the peptide bonds and formation of purple-colored (absorbance at 562 nm) complexes between Cu^{1+} and BCA (**Noble and Bailey, 2009**). The concentration of gelatin nanoparticles was measured only by BCA assay because Coomassie dye poorly binds to gelatin (Fig. S12).

The concentration of protein nanoparticles is usually measured by dye-based assays directly (in purified nanoparticles) or indirectly (in supernatants). We found out that the direct

method leads to sufficient underestimation (more than 50%) of BSA nanoparticles concentration (Table 5) compared to other methods. Noteworthy, the situation was completely different when analyzing heat-treated (NP6 and NP7) or partially cross-linked nanoparticles (NP11). The concentration of gelatin nanoparticles (NP8 and NP9) measured by direct BCA assay was higher than those obtained by other methods. These differences can be explained by a slower reaction of dyes with BSA molecules forming nanoparticles than with free BSA molecules. We suggested that a certain amount of time is necessary for Coomassie dye or copper ions to reach inner parts of the protein nanoparticle; therefore, it takes longer to complete the reaction.

To confirm this hypothesis, we incubated serial dilutions of pure BSA, gelatin, and nanoparticles cross-linked by different methods with BCA reagent for prolonged periods of time (up to 110 min). Calibration curves were recorded every 10 min (Fig. 8). The manufacturer's standard protocol prescribes the assessment of results after 30 min of incubation at +37 °C. Significantly slower growth of absorbance at 562 nm was observed for NP3, which were cross-linked with the excess of glutaraldehyde in comparison with NP6 and NP11. After that, we performed Bradford assay and BCA assay of NP3 and NP6 at +37 °C and +60 °C. We estimated the concentration of nanoparticles at different time intervals (Fig. S7). The concentration of NP6 was close to that determined by gravimetric analysis even at the first time point, and only slow growth was further observed. On the contrary, the concentration of NP3 was very low at the beginning of the experiment; however, then the substantial increase was observed. Despite that, even when the reaction was 2-3 times longer than standard protocols, concentration did not reach values comparable with the results of gravimetric analysis. Moreover, we destroyed NP2, NP4, and NP12 nanoparticles by alkaline hydrolysis, which led to an increase of signal in BCA and Bradford assays compared to intact nanoparticles and nanoparticles mixed with alkali before the assay (Fig. S8). These results confirm that excessively cross-linked nanoparticles react with dyes less intensively in comparison with pure protein.

The reaction of BCA reagent with heat-stabilized BSA nanoparticles, gelatin nanoparticles, and BSA nanoparticles with 40% cross-linking was substantially faster, indicating the role of cross-linking type and degree. Note that these nanoparticles were more susceptible to proteolytic degradation, which also depends on the cross-linking degree (Fig. 6). Therefore, protein nanoparticles with a high cross-linking degree can require prolonged incubation when protein concentration is measured by the direct method. Our findings are in agreement with previous reports showing that drugs released slower from HSA nanoparticles with a higher cross-linking degree (**Mo, 2007**, **Chen, 2010**).

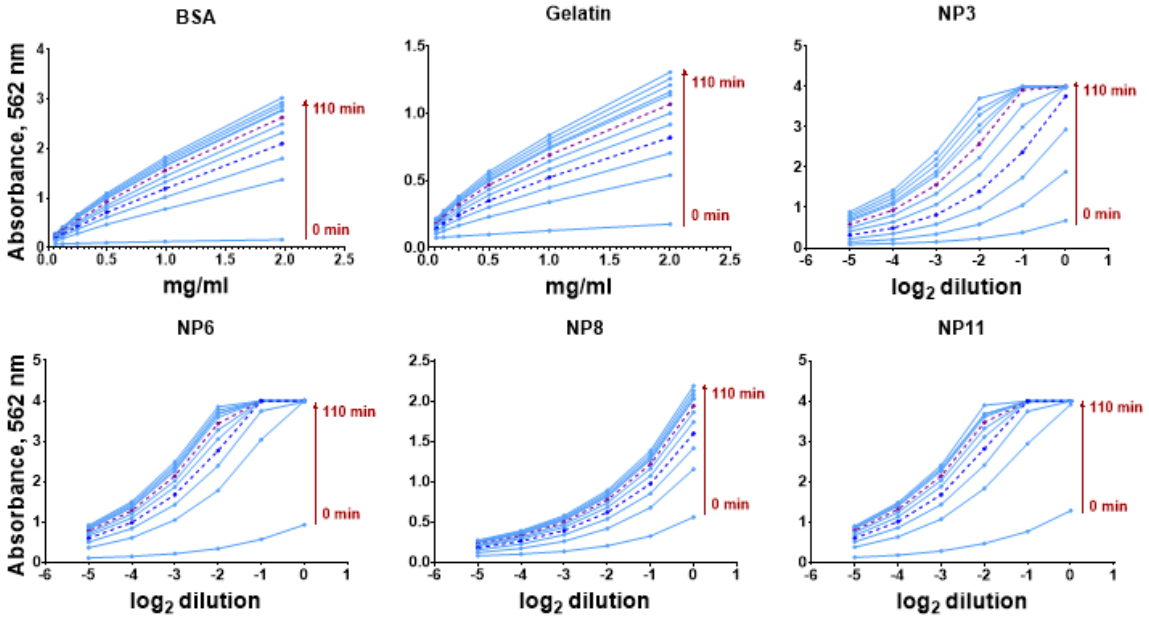

Fig. 8. BCA assay dose-response curves recorded in 10-minutes time intervals. Blue and purple dashed lines are dose-response curves at 30 and 60 min respectively.

Another data that reaffirm the effect of nanoparticles' presence on the results of dye-binding protein assays were obtained when the concentration of protein in desolvated samples was measured. We measured the concentration of BSA after desolvation and addition of glutaraldehyde (Table S6). Concentrations of protein after desolvation was more than two-fold lower than the expected value, except for batches NP6, NP7, and NP11. Unfortunately, desolvated gelatin quickly aggregated upon storage and was unsuitable for protein assay. Observed differences were not associated with the presence of glutaraldehyde and ethanol in desolvated samples because these chemicals increase the absorbance (see section 3.6.).

Concentrations of purified BSA nanoparticles measured by Bradford assay were generally lower than those obtained with BCA assay (except for batch NP13). The possible explanation is slower diffusion of Coomassie blue in the cross-linked BSA network compared to copper ions due to its larger size.

Concentrations of gelatin nanoparticles measured by direct BCA assay were higher than obtained with other methods. This may be due to the higher intensity of light scattering by gelatin nanoparticles, which have a larger diameter in comparison with BSA nanoparticles (Table 3 and Fig. S15). We did not perform light scattering correction because turbidity of protein nanoparticle solutions decreased after incubation with BCA reagent.

Arroyo-Maya et al. (**Arroyo-Maya, 2014**) showed that results of direct detection of protein in α-lactalbumin nanoparticles suspension by Kjeldahl assay (reference method) and BCA assay (assay was performed at +60 °C for 15 min) were almost equal. They synthesized nanoparticles with cross-linking degrees of 180% but did not observe significant underestimation of nanoparticle concentration. Considering that both proteins contain 10-11% of lysine (**Heine, 1991**), the number of intermolecular cross-links should be large for both BSA and α-LA nanoparticles. Evidently, α-lactalbumin nanoparticles quickly react with BCA reagent despite multiple cross-links. Possible reasons are higher reaction temperature, accelerating diffusion of copper ions through nanoparticles, and the difference in packing density of BSA (66 kDa) and α-lactalbumin (14 kDa). In carried experiments, though, direct BCA assay underestimated the concentration of excessively cross-linked BSA nanoparticles even at elevated temperature and prolonged incubation (Fig. S7).

3.6. BCA and Bradford protein assays: the indirect method

Quantification of non-desolvated protein in supernatants by BCA and Bradford assays (indirect approach) is widely used to determine the concentration of protein nanoparticles. In contrast to the results of the direct method, concentrations measured by indirect method and gravimetric analysis are comparable (Table 5). During the indirect assay performance, BSA calibration curves were constructed, taking into account that concentrations of pure BSA measured by absorbance at 280 nm and gravimetrically were different (see section 3.2.). Generally, concentrations were higher when determined by indirect BCA and Bradford assay in relation to BSA concentrations measured by gravimetric analysis due to substantial difference between initial BSA concentrations (e.g., 207,2 mg by UV280 versus 236,12 mg by gravimetry for BSA from "VWR"). Interestingly, the color of supernatants corresponded with the concentration of non-desolvated protein (Fig. S9)

We revealed the relationship (Fig. 9) between the yield of BSA nanoparticles and the difference of concentrations measured by BCA or Bradford assay and gravimetric analysis: the lower the synthesis yield, the higher overestimation of the nanoparticles concentration (BCA assay: Pearson r^2=0,7211, r=-0.8492, 95% CI from -0,9721 to -0,3598, p=0,0076, Bradford assay: Pearson r^2=0,6473, r=-0.8046, 95% CI from -0,9632 to -0,2307, p=0,0160). In this analysis, only batches prepared using excessive glutaraldehyde cross-linking were included. For several batches (NP5, NP10, and NP12), the difference was 20% and more. On the other hand, for batch NP13 (yield as low as 56%), the difference is lower than 20%.

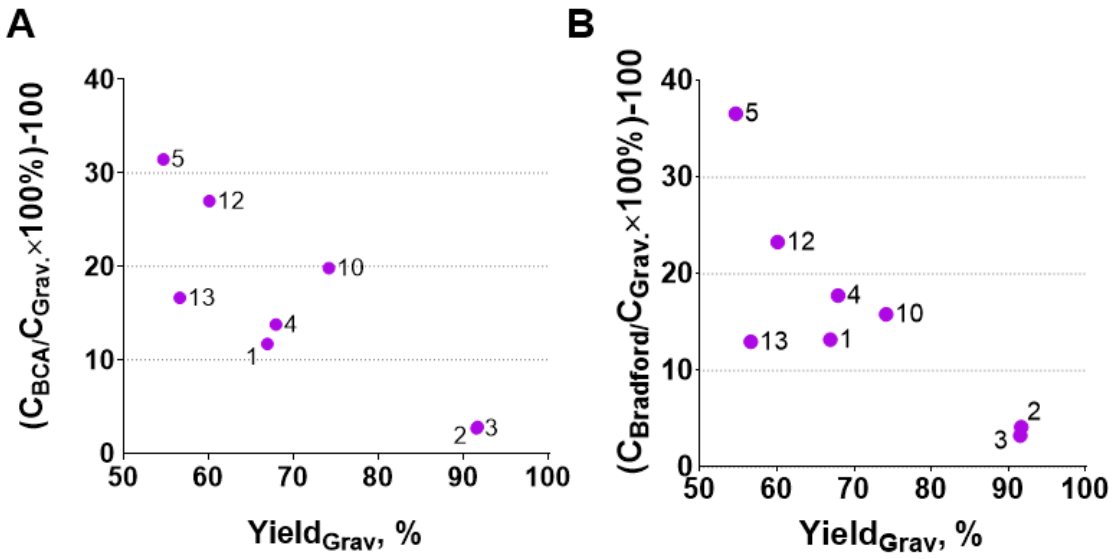

Fig. 9. Relationship between yield of synthesis and percentage difference of concentrations measured by indirect BCA (A) or Bradford assay (B) and gravimetric analysis. BSA calibration curves in BCA assay and Bradford assay were constructed using BSA concentration measured by gravimetric analysis. Point labels are numbers of BSA NP batches. C_{BSA} - concentration of BSA measured by indirect method, $C_{GRAV.}$ - concentration of BSA measured gravimetrically, $Yield_{GRAV}$ - yield of BSA nanoparticles estimated using C_{GRAV}

We attributed the difference between indirect dye-binding assays and gravimetric analysis to the presence of small BSA nanoparticles in supernatants, which were not removed by centrifugation and slowly react with Coomassie dye and copper ions (see the explanation at the beginning of this section). Supernatants after the first wash were analyzed by SDS-PAGE (Fig.

S5, S6A,B,D). Aggregates of BSA are located at the top of the gel (Fig. S6C), and their amount generally corresponds to the yield of nanoparticles.

We centrifuged desolvated BSA at 20000 g for 30 min. In these conditions, relatively clear supernatants and dense pellets of nanoparticles were formed. Perhaps, centrifugation at 20000 g does not allow sedimentation of small nanoparticles (tens of nanometers). At low nanoparticle yields, the percentage of such small nanoparticles and aggregates can be sufficient to influence the results of dye-binding assays. The presence of these nanoparticles leads to the underestimation of BSA concentration in supernatants and, consequently, to overestimation of purified nanoparticle concentration. In literature, different centrifugation conditions of BSA/HSA nanoparticles are reported: 6000 g for 5 min (**Tarhini, 2018**), 16000 g for 20 min (**Yedomon, 2013**), 16000 g for 10 min for particles of 140 nm, and 20000 g for smaller particles (**Von Storp, 2012**), 20000 g for 30 min (**Jun, 2011**), 20817 g for 10 min (**Wacker, 2011**), 25000 g for 30 min (**Ko and Gunasekaran, 2006**), 41000g for 20 min (**Luis de Redín, 2018**), 105000 g for 40 min (**Weber, 2000**). Most of the researchers centrifuged nanoparticles at 20000-25000 g and below. The amount of non-desolvated protein can also depend on desolvation duration. Standard protocol requires 24-hour-long incubation (**Weber, 2000**) while we cross-linked nanoparticles only or 60 min. However, analysis of literature data (Table S5) shows that the yield of nanoparticle synthesis to a greater extent depends on desolvation conditions (pH, ionic strength, initial protein concentration) rather than the duration of this process.

Other possible sources of incorrect results during indirect Bradford and BCA assays are turbidites of supernatant samples and the influence of cross-linkers and desolvating agents on the color development. The turbidity of supernatants depended on the cross-linking type and overall efficiency of desolvation. As can be seen from Fig. S9 and Table S7 the highest turbidity was for supernatants from batches NP1, NP5-9, and NP12. Although in indirect BCA and Bradford assays, we analyzed supernatants in dilutions 1:9 and 1:27 (lower dilutions' absorbances were beyond the calibration curve), light scattering could lead to an increase of absorbance at 562 nm or 595 nm and, consequently, to overestimation of protein concentration in supernatant. As we mentioned before, light scattering correction was not performed because samples' turbidity changed during incubation with dyes.

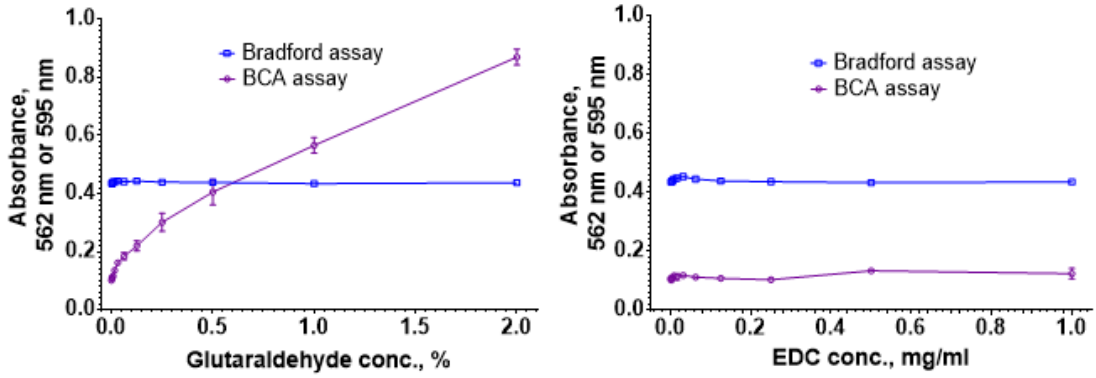

Fig. 10. Influence of EDC and glutaraldehyde on BCA and Bradford assays

Well known that various chemicals (including ethanol and glutaraldehyde) can affect the results of dye-binding protein assays (**Noble and Bailey, 2009**). We studied the influence of glutaraldehyde and another popular cross-linker, EDC, on the results of BCA and Bradford assays (Fig. 10). As expected, glutaraldehyde interferes with BCA assay due to its ability to reduce copper ions (**Tyllianakis, 1994**). The presence of 8-10% ethanol and 0,025% glutaraldehyde (which corresponds to 1:10 dilution of supernatant) leads to an overestimation of protein

concentration in BCA assay for both gelatin and BSA (Fig. S10, S12 and Table S8). Some irreproducible effect on Bradford assay was also detected (Fig. S11, S12 and Table S9). We should note that the interference strength of glutaraldehyde and ethanol depends on their concentration. In this work, glutaraldehyde was added to a great extent: 5,4 aldehyde groups per 1 lysine residue, which is 2.7-fold higher than typically used (**Langer, 2003**). In a previous study, Weber et al. found out that interference of free glutaraldehyde in the nanoparticles' supernatants with the BCA assay was negligible (**Weber, 2000**). Cross-linking degree in that paper was equal or lower than 2 aldehyde groups per 1 lysine residue.

Heating also has some effect on dye-binding assays. It is known that protein denaturation increases its reductive activity (**Mirsky and Anson, 1936**). Heating BSA at +70 °C for 120 min leads to the denaturation of most of the molecules (**Borzova, 2016**). In this regard, it can be expected that the absorption of a heated BSA should be higher than that of an unheated one; however, a slight decrease of absorbance in heated samples was observed in BCA assay, but not in Bradford assay (Fig. S13).

The combination of the described factors explains the differences in the concentrations between batches NP6-9 and NP11, measured using gravimetry and the indirect Bradford or BCA assay. Supernatants of batches NP8 and NP9 had the highest turbidity and scattered more light. The supernatant of NP11 contained less glutaraldehyde; thus, its interference was lower in comparison with batches NP1-5, NP10, and NP12-13.

3.7. Gravimetric analysis

Gravimetric analysis is the most straightforward method for protein nanoparticle quantification. We dried nanoparticles in porcelain crucibles at +140 °C to constant weight. The drying temperature was chosen according to TGA curves of gelatin and BSA nanoparticles (Fig. S14). No weight loss was observed until approximately +250 °C. According to the results of Kasarda and Black (**Kasarda and Black, 1968**), thermal decomposition of protein gradually increases from +130-150 °C and becomes more intense from +180-200 °C. We chose a drying temperature close to these values to remove the maximum possible amount of bound water. Standard conditions for determining protein dry weight are heating at +105 °C (**Kupke and Dorrier, 1978**). In the literature, the yield of nanoparticles is often determined using gravimetric analysis; however, conditions of analysis are rarely specified. In some papers, drying temperature as low as +60 °C (**Ofokansi, 2010**) and +80 °C (**Zhaparova, 2012**) was reported. It is difficult to assess to what extent heating temperature can affect the analysis results, but it should also be taken into account since it is known that heating temperature influences the amount of detected residual moisture (**Bradley, 2010**).

Two batches of concentrated gelatin (NP9) and BSA (NP10) nanoparticles were prepared for TGA. Concentrated samples were required due to the low crucible capacity (maximum volume is approximately 100 µL). We compared results of the gravimetric analysis with concentrations calculated from TGA curves and revealed that both concentrations matched perfectly for NP10 (123 mg/mL by gravimetry and 125,7 mg/mL by TGA), but not for NP9 (18,6 mg/mL by gravimetry and 21,2 mg/mL by TGA). The low concentration of gelatin nanoparticles can explain differences in results generated by both methods for NP9. Only approximately 2 mg of nanoparticles presented in 100 µL of nanoparticle suspension added to TGA crucible, which is too low for accurate measurement.

We should also note that the weight of glutaraldehyde bound to protein molecules was not considered when comparing the results of gravimetric analysis and other methods. Each BSA molecule has 59 lysine residues; each of them theoretically can react with one molecule of glutaraldehyde. Reaction with 59 glutaraldehyde molecules can increase each BSA molecule's weight by 5900 kDa (i.e., by 8-9%). Due to the presence of cross-links and free amine groups in

glutaraldehyde-treated BSA nanoparticles (**Weber, 2000**), it is hardly possible to calculate an accurate amount of glutaraldehyde molecules bound to a single BSA molecule.

3.8. Hydrolysis and UV absorbance

Measuring UV absorbance is a common protein quantification method; it is not surprising that it is often used to estimate protein nanoparticle concentration. In some papers, the concentration of nanoparticles in suspension was determined by direct assessment of absorbance at 280 nm (**Lomis, 2016**, **Sánchez-Segura, 2018**, **Tazhbayev, 2019**) or by indirect measurement of protein content in supernatants after washing of nanoparticles (**Wang, 2014**). We suppose that both approaches can lead to erroneous results for two reasons. The first reason is that the protein nanoparticles scatter light, which further increases absorbance (Fig. S15). This issue was addressed by Arroyo-Maya et al. (**Arroyo-Maya, 2014**) by applying the correction for light scattering. Despite this correction, the concentration of α-lactalbumin nanoparticles determined by UV absorbance was 60% higher than the concentration determined by the Kjeldahl assay (reference method). The possible explanation of this difference and the second source of incorrect results is that proteins change absorbance after treatment with cross-linking agents.

Absorbance at 280 nm of both gelatin and BSA significantly increases after interaction with glutaraldehyde; moreover, the absorbance of reacted protein is greater than the sum of the absorbances of protein and glutaraldehyde separately (Fig. 11C). Another consequence of this phenomenon is the complexity of the preparation of calibration solutions. We prepared a 1 mg/mL solution of glutaraldehyde treated BSA in two ways. In the first case, we mixed concentrated (circa 50 mg/mL) BSA aqueous solution with an appropriate amount of glutaraldehyde, incubated for 1 hour, and diluted BSA to 1 mg/mL (Fig. 11D). In the second case, we added the corresponding amount of glutaraldehyde to a 1 mg/mL solution of BSA (Fig. 11C). The absorbance of glutaraldehyde-treated BSA prepared by the first method was significantly higher. The difference is because of the faster reaction between glutaraldehyde and protein in a concentrated solution. When we prepared calibrators of hydrolysis experiments, we performed reactions of BSA or gelatin with glutaraldehyde under the same conditions (duration, temperature) in which nanoparticles were synthesized (Fig. 11A,B). However, it is still difficult to reach the same degree of interaction between protein and cross-linker.

Another method for determining protein nanoparticle concentration is the combination of hydrolysis with a measurement of absorbance at 280 nm (**Merodio, 2001**, **Merodio, 2002**, **Parasaram, 2016**). In preliminary experiments, we optimized hydrolysis conditions. Hydrolysis was performed in 1M, 2M, and 4M solutions of HCl and NaOH for several days. We added 666 µL of 10 M HCl or NaOH to 1 mL of undiluted nanoparticles. Aggregation of nanoparticles occurred at all HCl concentrations (Fig. 12). The hydrolysis rate in NaOH was monitored by measuring absorbance at 280 nm and 600 nm. Hydrolysis was completed in 48 h at 4 M NaOH and in 96 h at 2 M NaOH. Note that both absorbances at 280 nm and 600 nm (turbidity) decreased (Fig. S16), emphasizing the effect of light scattering on the quantification of nanoparticles by UV absorbance. Absorbances of free BSA have not changed significantly in four days (**data not shown**).

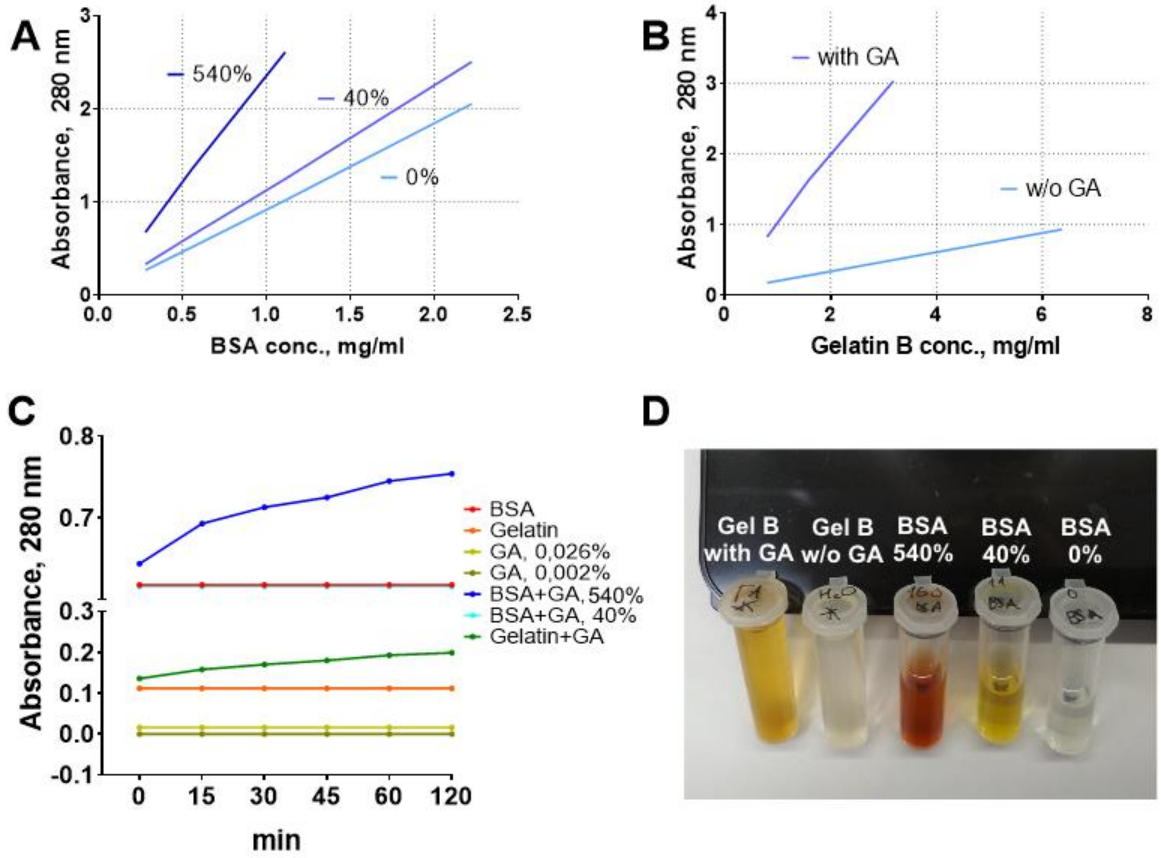

Fig. 11. A, B - absorbances of BSA (A) or gelatin B (B) treated with different amounts of glutaraldehyde after hydrolysis for 48 h in 4 M NaOH. C - changes in absorption of BSA, gelatin, glutaraldehyde, and glutaraldehyde-treated proteins over time (concentration of proteins is 1 mg/mL). D - solutions of BSA (50 mg/mL) and gelatin (26.6 mg/mL) treated with different amounts of glutaraldehyde. GA - glutaraldehyde. Percent shows an initial number of aldehyde groups per 100 lysine residues

We hydrolyzed BSA and gelatin nanoparticles in 4 M NaOH for two days. Calibration curves were constructed using BSA and gelatin treated with glutaraldehyde in conditions imitating those used during nanoparticle preparation (Fig. 11A,B). Heat-stabilized nanoparticles were quantified in relation to glutaraldehyde-untreated BSA. Concentrations determined by hydrolysis+UV were lower in comparison with results of gravimetric analysis and indirect dye-binding protein assays (Table 5) except for batches NP6, NP, and NP11. In preliminary tests, the concentration of nanoparticles determined by the hydrolysis method was only slightly lower than the concentration measured using gravimetric analysis. The reason for the discrepancy between the analysis results could be the peculiarities of the preparation of the calibration samples for nanoparticles cross-linked with an excess of glutaraldehyde described above. Indeed, batches NP6, NP, and NP11 were synthesized without the addition of glutaraldehyde or had a low cross-linking degree.

In the paper (**Merodio, 2001**), alkaline hydrolysis/UV and HPLC were used for measuring the concentration of BSA nanoparticles and gave similar results despite calibration solutions of BSA were prepared without the addition of glutaraldehyde. The authors used a low concentration of glutaraldehyde, 1.56 μg per 1 mg of HSA, whereas approximately 50 μg per 1 mg is necessary for 100% cross-linking (**Langer, 2003**). Such a low cross-linking degree should not lead to a significant absorbance change compared with intact protein (Fig. 11A).

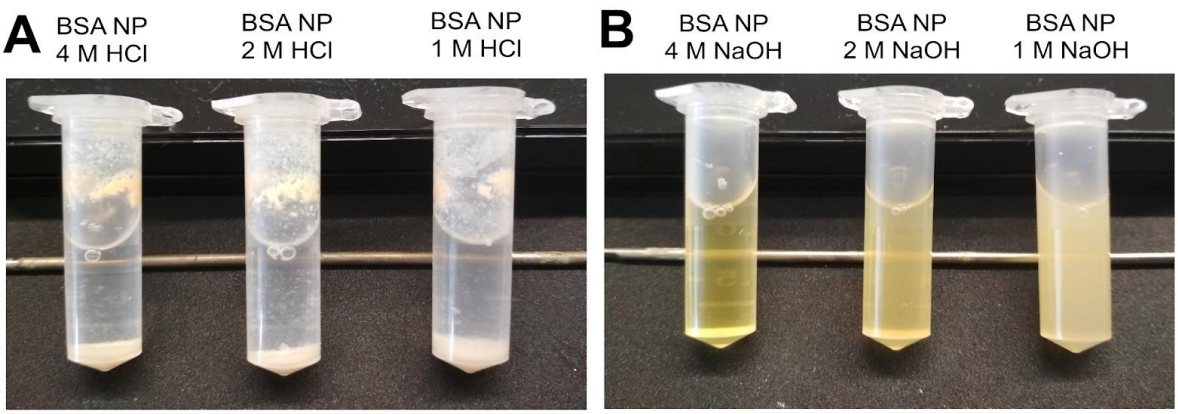

Fig. 12. BSA nanoparticles after incubation for 48 h in HCl and NaOH aqueous solutions with various concentrations at +37 °C

4. Conclusion

The main result of this work is that the nature of protein and assay conditions, as well as type and degree of cross-linking, influence the results of nanoparticle concentration measurement. It is especially true for direct dye-binding protein assays. We assume that high cross-linking intensity leads to slower diffusion of Coomassie dye and copper ions through nanoparticles' matrix. Therefore, more time is necessary for dye molecules and copper ions to reach all available protein molecules. The presence of nanoparticles in supernatants after desolvation is a source of incorrect results for indirect dye-binding assays, leading to underestimating non-desolvated protein. On the other hand, the presence of nanoparticles in supernatants increases absorbance through light scattering, which results in the overestimation of non-desolvated protein. The presence of the small nanoparticles in the supernatant can be an issue when there is no optimized desolvation protocol (e.g., when novel proteins, desolvating agents, or cross-linking approaches are tested). At a low cross-linking degree, the effect of diffusion slowdown is less pronounced and does not affect concentration measurements. Note that the number of cross-links depends on protein structure, the number of reactive amino acids per molecule, and the amount of cross-linker.

Interference of cross-linkers with dye-binding assays should also be taken into account. In recent papers, a lot of uncommon cross-linkers were reported: vanillin (**Li, 2016b**), ruthenium and ammonium persulfate (**Long, 2019**), cysteine (**Tazhbayev, 2019**), zinc ions (**Elgohary, 2018**), 3,3′-dithiobis [sulfosuccinimidylpropionate] (**Deng, 2018**). The application of innovative cross-linking approaches should be accompanied by checking whether they affect absorbance at certain wavelengths and binding of dyes to protein. Change of protein absorbance for different cross-linker to protein ratios should also be verified when spectroscopic methods to be used. Light scattering correction needs to be made when protein nanoparticles are quantified by direct measuring UV absorbance (**Arroyo-Maya, 2014**).

We can formulate the key recommendation to determine the concentration of protein nanoparticles by at least two different methods. In our opinion, straightforward gravimetric analysis is a good choice, especially when refined with TGA. Some residual moisture can present in protein nanoparticle samples even after drying at temperatures higher than +100 C; therefore, the application of TGA allows a more reliable estimation of dry weight. Accurate weighing of nanoparticles requires sufficient amounts of nanoparticles in terms of quantity and concentration, which depend on laboratory scales' accuracy and crucible volume (in the case of TGA).

Acknowledgements

Authors thank Dr. Ekaterina Khramtsova for her help with the mechanism of amide bond formation. The work was carried out using the equipment of the Core Facilities Center “Research of the materials and matter” at the PFRC UB RAS.

Funding

The reported study was funded by RFBR, project number 19-015-00408 A

Conflict of Interest

The authors declare that they have no conflict of interest

References

Altintas, I., Heukers, R., Van Der Meel, R., Lacombe, M., Amidi, M., Van Bergen En Henegouwen, P.M.P., Hennink, W.E., Schiffelers, R.M., Kok, R.J., 2013. Nanobody-albumin nanoparticles (NANAPs) for the delivery of a multikinase inhibitor 17864 to EGFR overexpressing tumor cells. J. Control. Release. 165, 110-118. DOI: 10.1016/j.jconrel.2012.11.007

Anders, J.C., Parten, B.F., Petrie, G.E., Marlowe, R.L., McEntire, J.E., 2003. Using amino acid analysis to determine absorptivity constants: A validation case study using bovine serum albumin. BioPharm Int. 16, 30-37.

Anhorn, M. G., Wagner, S., Kreuter, J., Langer, K., von Briesen, H., 2008. Specific Targeting of HER2 Overexpressing Breast Cancer Cells with Doxorubicin-Loaded Trastuzumab-Modified Human Serum Albumin Nanoparticles. Bioconjug. Chem. 19, 2321–2331. doi:10.1021/bc8002452

Arnedo, A., Irache, J.M., Merodio, M., Espuelas Millán, M.S., 2004. Albumin nanoparticles improved the stability, nuclear accumulation and anticytomegaloviral activity of a phosphodiester oligonucleotide. J. Controi. Release. 94, 217-227. DOI: 10.1016/j.jconrel.2003.10.009

Arroyo-Maya, I. J., Hernández-Sánchez, H., Jiménez-Cruz, E., Camarillo-Cadena, M., Hernández-Arana, A., 2014. α-Lactalbumin nanoparticles prepared by desolvation and cross-linking: Structure and stability of the assembled protein. Biophys. Chem. 193-194, 27–34. doi:10.1016/j.bpc.2014.07.003

Asghar, S., Salmani, J.M.M., Hassan, W., Xie, Y., Meng, F., Su, Z., Sun, M., Xiao, Y., Ping, Q., 2014. A facile approach for crosslinker free nano self assembly of protein for anti-tumor drug delivery: Factors' optimization, characterization and in vitro evaluation. Eur. J. Pharm. Sci. 63, 53-62. DOI: 10.1016/j.ejps.2014.06.022

Bhushan, B., Khanadeev, V., Khlebtsov, B., Khlebtsov, N., Gopinath, P., 2017. Impact of albumin based approaches in nanomedicine: Imaging, targeting and drug delivery. Adv. Colloid Interface Sci. 246, 13–39. doi:10.1016/j.cis.2017.06.012

Borzova, V.A., Markossian, K.A., Chebotareva, N.A., Kleymenov, S.Yu., Poliansky, N.B., Muranov, K.O., Stein-Margolina, V.A., Shubin, V.V., Markov, D.I., Kurganov, B.I., 2016. Kinetics of thermal denaturation and aggregation of bovine serum albumin. PLoS ONE. 11, e0153495. DOI: 10.1371/journal.pone.0153495

Bradley, R. L., 2010. Moisture and Total Solids Analysis, in: Nielsen, S. S. (Ed.), Food Analysis. Food Science Texts Series., Boston, pp. 85–104. doi:10.1007/978-1-4419-1478-1_6

Cai, B., Rao, L., Ji, X., Bu, L. L., He, Z., Wan, D., Yang, Y., Liu, W., Guo, S., Zhao, X. Z., 2016. Autofluorescent gelatin nanoparticles as imaging probes to monitor matrix metalloproteinase metabolism of cancer cells. J. Biomed. Mater. Res. A. 104, 2854–2860. doi:10.1002/jbm.a.35823

Chang, T.Z., Deng, L., Wang, B.Z., Champion, J.A., 2018. H7 Hemagglutinin nanoparticles retain immunogenicity after >3 months of 25°C storage. PLOS ONE. 13, e0202300. 10.1371/journal.pone.0202300

Chang, T.Z., Stadmiller, S.S., Staskevicius, E., Champion, J.A., 2017. Effects of ovalbumin protein nanoparticle vaccine size and coating on dendritic cell processing. Biomater. Sci. 5, 223-233. DOI: 10.1039/c6bm00500d

Chen, K., Wacker, M., Hackbarth, S., Ludwig, C., Langer, K., Röder, B., 2010. Photophysical evaluation of mTHPC-loaded HSA nanoparticles as novel PDT delivery systems. J.Photochem. Photobiol. B. 101, 340-347. DOI: 10.1016/j.jphotobiol.2010.08.006

Coester, C.J., Langer, K., van Briesen, H., Kreuter, J., 2000. Gelatin nanoparticles by two step desolvation--a new preparation method, surface modifications and cell uptake. J Microencapsul. 17, 187-193. doi:10.1080/026520400288427

Croguennec, T., Renault, A., Beaufils, S., Dubois, J., Pezennec, S., 2007. Interfacial properties of heat-treated ovalbumin. J. Colloid Interface Sci. 315, 627-636. DOI: 10.1016/j.jcis.2007.07.041

Deng, L., Mohan, T., Chang, T. Z., Gonzalez, G. X., Wang, Y., Kwon, Y.-M., Kang, S.M., Compans, R.W., Champion, J.A., Wang, B.-Z., 2018. Double-layered protein nanoparticles induce broad protection against divergent influenza A viruses. Nat. Commun. 9, 359. doi:10.1038/s41467-017-02725-4

Elgohary, M.M., Helmy, M.W., Mortada, S.M., Elzoghby, A.O., 2018. Dual-targeted nano-in-nano albumin carriers enhance the efficacy of combined chemo/herbal therapy of lung cancer. Nanomedicine. 13, 2221-2244. DOI: 10.2217/nnm-2018-0097

Elzoghby, A.O., Helmy, M.W., Samy, W.M., Elgindy, N.A., 2013. Novel ionically crosslinked casein nanoparticles for flutamide delivery: formulation, characterization, and in vivo pharmacokinetics. Int. J. Nanomedicine. 8, 1721-1732. doi:10.2147/IJN.S40674

Elzoghby, A.O., Samy, W.M., Elgindy, N.A., 2012. Albumin-based nanoparticles as potential controlled release drug delivery systems. J. Control. Release. 157, 168-182. DOI: 10.1016/j.jconrel.2011.07.031

Esposito, E., Cortesi, R., Nastruzzi, C., 1996. Gelatin microspheres: influence of preparation parameters and thermal treatment on chemico-physical and biopharmaceutical properties. Biomaterials. 17, 2009–2020. doi:10.1016/0142-9612(95)00325-8

Futami, J., Miyamoto, A., Hagimoto, A., Suzuki, S., Futami, M., Tada, H., 2017. Evaluation of irreversible protein thermal inactivation caused by breakage of disulphide bonds using methanethiosulphonate. Sci. Rep. 7, 12471. doi:10.1038/s41598-017-12748-y

Galisteo-González, F., Molina-Bolívar, J. A., 2014. Systematic study on the preparation of BSA nanoparticles. Colloid. Surface B. 123, 286–292. doi:10.1016/j.colsurfb.2014.09.028

Geh, K. J., Hubert, M., Winter, G., 2016. Optimisation of one-step desolvation and scale-up of gelatine nanoparticle production. J. Microencapsul. 33, 595–604. doi:10.1080/02652048.2016.1228706

Gerrard, J. A., 2002. Protein–protein crosslinking in food: methods, consequences, applications. Trends Food Sci. Technol. 13, 391–399. doi:10.1016/s0924-2244(02)00257-1

Ghoshdastidar, S., Gangula, A., Kainth, J., Saranathan, S., Elangovan, A., Afrasiabi, Z., Hainsworth, D.P., Upendran, A., Kannan, R., 2020. Plate-Adherent Nanosubstrate for Improved ELISA of Small Molecules: A Proof of Concept Study. Anal. Chem. 92, 10952-10956. DOI: 10.1021/acs.analchem.0c01441

Gilbert, J., Cheng, C. J., & Jones, O. G., 2017. Vapor Barrier Properties and Mechanical Behaviors of Composite Hydroxypropyl Methylcelluose/Zein Nanoparticle Films. Food Biophys. 13, 25–36. doi:10.1007/s11483-017-9508-1

Goswami, S., Thiyagarajan, D., Das, G., Ramesh, A., 2014. Biocompatible nanocarrier fortified with a dipyridinium-based amphiphile for eradication of biofilm. ACS Appl. Mater. Interfaces. 6, 16384-16394. DOI: 10.1021/am504779t

Gulzar, M., Bouhallab, S., Jeantet, R., Schuck, P., & Croguennec, T., 2011. Influence of pH on the dry heat-induced denaturation/aggregation of whey proteins. Food Chem. 129, 110–116. doi:10.1016/j.foodchem.2011.04.037

Guo, X., Cheng, Y., Zhao, X., Luo, Y., Chen, J., Yuan, W. E., 2018. Advances in redox-responsive drug delivery systems of tumor microenvironment. J. Nanobiotechnology. 16, 74. https://doi.org/10.1186/s12951-018-0398-2

Habibi, N., Christau, S., Ochyl, L.J., Fan, Z., Hassani Najafabadi, A., Kuehnhammer, M., Zhang, M., Helgeson, M., von Klitzing, R., Moon, J.J., Lahann, J., 2020. Engineered Ovalbumin Nanoparticles for Cancer Immunotherapy. Adv. Therap. 3, 2000100. doi:10.1002/adtp.202000100

Hafidz, R.N.R.M., Yaakob, C.M., Amin, I., Noorfaizan, A., 2011. Chemical and functional properties of bovine and porcine skin gelatin. Int. Food Res. J. 18, 813-817..

Hassanin, I.A., Elzoghby, A.O., 2020. Self-assembled non-covalent protein-drug nanoparticles: an emerging delivery platform for anti-cancer drugs. Expert Opin. Drug Del. 17, 1437-1458 DOI: 10.1080/17425247.2020.1813713

Havea, P., Singh, H., & Creamer, L. K., 2001. Characterization of heat-induced aggregates of β-lactoglobulin, α-lactalbumin and bovine serum albumin in a whey protein concentrate environment. J. Dairy Res. 68, 483-497. doi:10.1017/s0022029901004964

Heine, W. E., Klein, P. D., Reeds, P. J., 1991. The Importance of α-Lactalbumin in Infant Nutrition. J. Nutr. 121, 277–283. doi:10.1093/jn/121.3.277

Herrera Estrada, L. P., Champion, J. A., 2015. Protein nanoparticles for therapeutic protein delivery. Biomater. Sci. 3, 787–799. doi:10.1039/c5bm00052a

Heukers, R., Altintas, I., Raghoenath, S., De Zan, E., Pepermans, R., Roovers, R. C., Haselberg, R., Hennink, W. E., Schiffelers, R. M., Kok, R. J., van Bergen en Henegouwen, P. M. P., 2014. Targeting hepatocyte growth factor receptor (Met) positive tumor cells using internalizing nanobody-decorated albumin nanoparticles. Biomaterials. 35, 601–610. doi:10.1016/j.biomaterials.2013.10.001

Huang, D., Chen, Y.-S., Rupenthal, I.D., 2017. Hyaluronic acid coated albumin nanoparticles for targeted peptide delivery to the retina. Mol. Pharm. 14, 533-545. DOI: 10.1021/acs.molpharmaceut.6b01029

Huang, Y., Luo, Y., Zheng, W., Chen, T., 2014. Rational design of cancer-targeted BSA protein nanoparticles as radiosensitizer to overcome cancer radioresistance. ACS Appl. Mater. Interfaces. 6, 19217-19228. DOI: 10.1021/am505246w

Jahanban-Esfahlan, A., Dastmalchi, S., Davaran, S., 2016. A simple improved desolvation method for the rapid preparation of albumin nanoparticles. Int. J. Biol. Macromol. 91, 703-709. DOI: 10.1016/j.ijbiomac.2016.05.032

Jun, J. Y., Nguyen, H. H., Paik, S.-Y.-R., Chun, H. S., Kang, B.-C., Ko, S., 2011. Preparation of size-controlled bovine serum albumin (BSA) nanoparticles by a modified desolvation method. Food Chem. 127, 892–1898. doi:10.1016/j.foodchem.2011.02.040

Karami, K., Jamshidian, N., Hajiaghasi, A., Amirghofran, Z., 2020. BSA nanoparticles as controlled release carriers for isophethalaldoxime palladacycle complex; Synthesis, characterization,: In vitro evaluation, cytotoxicity and release kinetics analysis. New J. Chem. 44, 4394-4405. DOI: 10.1039/c9nj05847h

Kasarda, D.D., Black, D.R., 1968. Thermal degradation of proteins studied by mass spectrometry. Biopolymers. 6, 1001-4. doi: 10.1002/bip.1968.360060712.

Kommareddy, S., Amiji, M. M., 2008. Preparation and Loading of Gelatin Nanoparticles. Cold Spring Harb. Protoc. 2008, pdb.prot4885–pdb.prot4885. doi:10.1101/pdb.prot4885

Kumar, S., Meena, R., Rajamani, P., 2016. Fabrication of BSA-Green Tea Polyphenols-Chitosan Nanoparticles and Their Role in Radioprotection: A Molecular and Biochemical Approach. J. Agric. Food Chem. 64, 6024-6034. DOI: 10.1021/acs.jafc.6b02068

Kupke, D.W., Dorrier, T.E., 1978. Protein concentration measurements: the dry weight. Method. Enzymol. 48, 155-62. doi: 10.1016/s0076-6879(78)48008-5

Lambrecht, M.A., Rombouts, I., Delcour, J.A., 2016. Denaturation and covalent network formation of wheat gluten, globular proteins and mixtures thereof in aqueous ethanol and water. Food Hydrocoll. 57, 122-131. DOI: 10.1016/j.foodhyd.2016.01.018

Langer, K., Anhorn, M.G., Steinhauser, I., Dreis, S., Celebi, D., Schrickel, N., Faust, S., Vogel, V., 2008. Human serum albumin (HSA) nanoparticles: Reproducibility of preparation process and kinetics of enzymatic degradation. Int. J. Pharm. 347, 109-117. DOI: 10.1016/j.ijpharm.2007.06.028

Langer, K., Balthasar, S., Vogel, V., Dinauer, N., Von Briesen, H., Schubert, D., 2003. Optimization of the preparation process for human serum albumin (HSA) nanoparticles. Int. J. Pharm. 257, 169-180. DOI: 10.1016/S0378-5173(03)00134-0

Lee, M. J., Lee, E. S., Kim, T. H., Jeon, J. W., Kim, Y., Oh, B. K., 2019. Detection of thioredoxin-1 using ultra-sensitive ELISA with enzyme-encapsulated human serum albumin nanoparticle. Nano Converg. 6, 37. https://doi.org/10.1186/s40580-019-0210-5

Li, F., Jiang, L., Xin, J., Zheng, C., Zhu, J., Liu, J., 2016. Preparation and in vitro evaluation of albumin nanoparticles produced by thermal driven self-assembly. J. China Pharm. Univ. 47, 303-310. DOI: 10.11665/j.issn.1000-5048.20160310

Li, F., Zheng, C., Xin, J., Chen, F., Ling, H., Sun, L., Webster, T.J., Ming, X., Liu, J., 2016. Enhanced tumor delivery and antitumor response of doxorubicin-loaded albumin nanoparticles formulated based on a schiff base. Int. J. Nanomedicine. 11, 3875-3890. DOI: 10.2147/IJN.S108689

Li, X., Mu, J., Liu, F., Tan, E.W.P., Khezri, B., Webster, R.D., Yeow, E.K.L., Xing, B., 2015. Human transport protein carrier for controlled photoactivation of antitumor prodrug and real-time intracellular tumor imaging. Bioconjug. Chem. 26, 955-961. DOI: 10.1021/acs.bioconjchem.5b00170

Liu, G., Lin, Y., Ostatná, V., Wang, J., 2005. Enzyme nanoparticles-based electronic biosensor. Chemical Communications. 27, 3481-3483. doi:10.1039/b504943a

Liu, J., Xing, X., Jing, H., 2018. Differentiation of glycated residue numbers on heat-induced structural changes of bovine serum albumin. J. Sci. Food Agric. 98, 2168-2175. DOI: 10.1002/jsfa.8701

Lomis, N., Westfall, S., Farahdel, L., Malhotra, M., Shum-Tim, D., Prakash, S., 2016. Human Serum Albumin Nanoparticles for Use in Cancer Drug Delivery: Process Optimization and In Vitro Characterization. Nanomaterials. 6, 116. doi:10.3390/nano6060116

Long, X., Ren, J., Zhang, C., Ji, F., Jia, L., 2019. Facile and controllable fabrication of protein-only nanoparticles through photo-induced crosslinking of albumin and their application as dox carriers. Nanomaterials. 9, 797. DOI: 10.3390/nano9050797

Luebbert, C.C., Clarke, T.M., Pointet, R., Frahm, G.E., Tam, S., Lorbetskie, B., Sauvé, S., Johnston, M.J.W., 2017. Nanoparticle size and production efficiency are affected by the presence of fatty acids during albumin nanoparticle fabrication. PLoS ONE. 12, e0189814. DOI: 10.1371/journal.pone.0189814

Luis de Redín, I., Boiero, C., Martínez-Ohárriz, M. C., Agüeros, M., Ramos, R., Peñuelas, I., Allemandi, D., Llabot, J. M., Irache, J. M., 2018. Human serum albumin nanoparticles for ocular delivery of bevacizumab. Int. J. Pharm. 541, 214–223.

Ma, X., Sun, X., Hargrove, D., Chen, J., Song, D., Dong, Q., Lu, X., Fan, T.-H., Fu, Y., Lei, Y. A., 2016. Biocompatible and Biodegradable Protein Hydrogel with Green and Red Autofluorescence: Preparation, Characterization and in Vivo Biodegradation Tracking and Modeling. Sci. Rep. 6, 19370. DOI: 10.1038/srep19370

Martins, J. T., Bourbon, A. I., Pinheiro, A. C., Fasolin, L. H., Vicente, A. A., 2018. Protein-Based Structures for Food Applications: From Macro to Nanoscale. Front. Sustain. Food Syst. 2, 77. doi:10.3389/fsufs.2018.00077

Merodio, M., Arnedo, A., Renedo, M. J., Irache, J. M., 2001. Ganciclovir-loaded albumin nanoparticles: characterization and in vitro release properties. Eur. J. Pharm. Sci. 12, 251–259. doi:10.1016/s0928-0987(00)00169-x

Merodio, M., Irache, J. M., Valamanesh, F., Mirshahi, M., 2002. Ocular disposition and tolerance of ganciclovir-loaded albumin nanoparticles after intravitreal injection in rats. Biomaterials, 23, 1587–1594. doi:10.1016/s0142-9612(01)00284-8

Migneault, I., Dartiguenave, C., Bertrand, M.J., Waldron, K.C., 2004. Glutaraldehyde: Behavior in aqueous solution, reaction with proteins, and application to enzyme crosslinking. BioTechniques,.37, 790-802. DOI: 10.2144/04375rv01

Mine, Y., 1995. Recent advances in the understanding of egg white protein functionality. Trends Food Sci. Tech. 6, 225-232. DOI: 10.1016/S0924-2244(00)89083-4

Mirsky, A.E., Anson, M.L., 1936. The reducing groups of proteins. J. Gen. Physiol. 19, 451-459. DOI: 10.1085/jgp.19.3.451

Mo, Y., Barnett, M. E., Takemoto, D., Davidson, H., Kompella, U. B., 2007. Human serum albumin nanoparticles for efficient delivery of Cu, Zn superoxide dismutase gene. Mol. Vis, 13, 746–757.

Neelam, Chhillar, A.K., Rana, J.S., 2019. Enzyme nanoparticles and their biosensing applications: A review. Anal. Biochem. 581, 113345. DOI: 10.1016/j.ab.2019.113345

Noble, J.E., Bailey, M.J., 2009. Quantitation of protein. Method. Enzymol. 463, 73-95. doi: 10.1016/S0076-6879(09)63008-1.

Ofokansi, K., Winter, G., Fricker, G., & Coester, C., 2010. Matrix-loaded biodegradable gelatin nanoparticles as new approach to improve drug loading and delivery. Eur. J. Pharm. Biopharm. 76, 1–9. doi:10.1016/j.ejpb.2010.04.008

Pace, C.N., Vajdos, F., Fee, L., Grimsley, G., Gray, T., 1995. How to measure and predict the molar absorption coefficient of a protein. Protein Sci. 4, 2411-2423. DOI: 10.1002/pro.5560041120

Pan, H., Li, S., Li, M., Tao, Q., Jia, J., Li, W., Wang, L., Guo, Z., Ma, K., Liu, Y., Cui, C., 2020. Anti-CD19 mAb-conjugated human serum albumin nanoparticles effectively deliver doxorubicin to B-lymphoblastic leukemia cells. Pharmazie. 75, 318-323. DOI: 10.1691/ph.2020.0026

Parasaram, V., Nosoudi, N., LeClair, R.J., Binks, A., Vyavahare, N., 2016. Targeted drug delivery to emphysematous lungs: Inhibition of MMPs by doxycycline loaded nanoparticles. Pulm. Pharmacol. Ther. 39, 64-73. DOI: 10.1016/j.pupt.2016.06.004.

Peña, I., Domínguez, J. M., 2010. Thermally Denatured BSA, a Surrogate Additive to Replace BSA in Buffers for High-Throughput Screening. J. Biomol. Screen. 15, 1281–1286. doi:10.1177/1087057110379768

Pustulka, S. M., Ling, K., Pish, S. L., Champion, J. A., 2020. Protein Nanoparticle Charge and Hydrophobicity Govern Protein Corona and Macrophage Uptake. ACS Appl. Mater. Interfaces. 12, 48284–48295. doi:10.1021/acsami.0c12341

Rombouts, I., Lagrain, B., Scherf, K. A., Lambrecht, M. A., Koehler, P., Delcour, J. A., 2015. Formation and reshuffling of disulfide bonds in bovine serum albumin demonstrated using tandem mass spectrometry with collision-induced and electron-transfer dissociation. Sci. Rep. 5, 12210. https://doi.org/10.1038/srep12210

Sánchez-Segura, L., Ochoa-Alejo, N., Carriles, R., Zavala-García, L. E., 2018. Development of bovine serum albumin–capsaicin nanoparticles for biotechnological applications. Appl. Nanosci. 8, 1877–1886. doi:10.1007/s13204-018-0874-x

Stamey, T.A., Teplow, D.B., Graves, H.C.B., 1995. Identity of PSA purified from seminal fluid by different methods: Comparison by amino acid analysis and assigned extinction coefficients. The Prostate. 27, 198-203. DOI: 10.1002/pros.2990270404

Tan, H., Sun, G., Lin, W., Mu, C., Ngai, T., 2014. Gelatin Particle-Stabilized High Internal Phase Emulsions as Nutraceutical Containers. ACS Appl. Mater. Interfaces. 6, 13977–13984. doi:10.1021/am503341j

Tan, H., Tu, Z., Jia, H., Gou, X., Ngai, T., 2018. Hierarchical Porous Protein Scaffold Templated from High Internal Phase Emulsion Costabilized by Gelatin and Gelatin Nanoparticles. Langmuir. 34, 4820–4829. doi:10.1021/acs.langmuir.7b04047

Tarhini, M., Benlyamani, I., Hamdani, S., Agusti, G., Fessi, H., Greige-Gerges, H., Bentaher, A., Elaissari, A., 2018. Protein-Based Nanoparticle Preparation via Nanoprecipitation Method. Materials. 11, 394. doi.org/10.3390/ma11030394

Tazhbayev, Y., Mukashev, O., Burkeev, M., Kreuter, J., 2019. Hydroxyurea-loaded albumin nanoparticles: Preparation, characterization, and in vitro studies. Pharmaceutics. 11, 410. DOI: 10.3390/pharmaceutics11080410

Tyllianakis, P. E., Kakabakos, S. E., Evangelatos, G. P., Ithakissios, D. S., 1994. Direct Colorimetric Determination of Solid-Supported Functional Groups and Ligands Using Bicinchoninic Acid. Anal. Biochem. 219, 335–340. doi:10.1006/abio.1994.1273

Varca, G. H. C., Ferraz, C. C., Lopes, P. S., Mathor, M. B., Grasselli, M., Lugão, A. B., 2014. Radio-synthesized protein-based nanoparticles for biomedical purposes. Radiat. Phys. Chem. 94, 181–185. doi:10.1016/j.radphyschem.2013.05.057

Von Storp, B., Engel, A., Boeker, A., Ploeger, M., Langer, K., 2012. Albumin nanoparticles with predictable size by desolvation procedure. J. Microencapsul. 29, 138–146. doi:10.3109/02652048.2011.635218

Wacker, M., Zensi, A., Kufleitner, J., Ruff, A., Schütz, J., Stockburger, T., Marstaller, T., Vogel, V., 2011. A toolbox for the upscaling of ethanolic human serum albumin (HSA) desolvation. Int. J. Pharm. 414, 225–232. doi:10.1016/j.ijpharm.2011.04.046

Wang, L., Hess, A., Chang, T. Z., Wang, Y.-C., Champion, J. A., Compans, R. W., Wang, B.-Z., 2014. Nanoclusters self-assembled from conformation-stabilized influenza M2e as broadly cross-protective influenza vaccines. Nanomedicine. 10, 473-482. doi:10.1016/j.nano.2013.08.005

Wang, W., Huang, Y., Zhao, S., Shao, T., Cheng, Y., 2013. Human serum albumin (HSA) nanoparticles stabilized with intermolecular disulfide bonds. Chem. Commun. 49, 2234-2236. doi:10.1039/c3cc38397k

Wang, Y., Deng, L., Gonzalez, G.X., Luthra, L., Dong, C., Ma, Y., Zou, J., Kang, S.-M., Wang, B.-Z., 2020. Double-Layered M2e-NA Protein Nanoparticle Immunization Induces Broad Cross-Protection against Different Influenza Viruses in Mice. Adv. Healthc. Mater., 9, 1901176. DOI: 10.1002/adhm.201901176

Wang, Y., Deng, L., Kang, S.-M., Wang, B.-Z., 2018. Universal influenza vaccines: from viruses to nanoparticles. Expert Rev. Vaccines. 17, 967-976. DOI: 10.1080/14760584.2018.1541408

Wang, Z., Dong, L., Han, L., Wang, K., Lu, X., Fang, L., Qu, S., Chan, C. W., 2016. Self-assembled Biodegradable Nanoparticles and Polysaccharides as Biomimetic ECM Nanostructures for the Synergistic effect of RGD and BMP-2 on Bone Formation. Sci. Rep. 6, 25090. doi:10.1038/srep25090

Weber, C., Coester, C., Kreuter, J., Langer, K., 2000. Desolvation process and surface characterisation of protein nanoparticles. Int. J. Pharm. 194, 91–102. doi:10.1016/s0378-5173(99)00370-1

Wei, W., Wang, L.-Y., Yuan, L., Wei, Q., Yang, X.-D., Su, Z.-G., Ma, G.-H., 2007. Preparation and application of novel microspheres possessing autofluorescent properties. Adv. Funct. Mater. 17, 3153-3158. DOI: 10.1002/adfm.200700274

Woods, A., Patel, A., Spina, D., Riffo-Vasquez, Y., Babin-Morgan, A., de Rosales, R. T., Sunassee, K., Clark, S., Collins, H., Bruce, K., Dailey, L. A., Forbes, B., 2015. In vivo biocompatibility, clearance, and biodistribution of albumin vehicles for pulmonary drug delivery. J. Control. Release. 210, 1–9. DOI: 10.1016/j.jconrel.2015.05.269

Xu, J., Wang, J., Luft, J.C., Tian, S., Owens, G., Pandya, A.A., Berglund, P., Pohlhaus, P., Maynor, B.W., Smith, J., Hubby, B., Napier, M.E., Desimone, J.M., 2012. Rendering protein-based particles transiently insoluble for therapeutic applications. J. Am. Chem. Soc. 134, 8774-8777. DOI: 10.1021/ja302363r

Yaman, Y.T., Akbal, O., Abaci, S., 2019. Development of clay-protein based composite nanoparticles modified single-used sensor platform for electrochemical cytosensing application. Biosens. Bioelectron. 132, 230-237. DOI: 10.1016/j.bios.2019.02.058

Yang, Q., Ye, Z., Zhong, M., Chen, B., Chen, J., Zeng, R., Wei, L., Li, H. W., Xiao, L., 2016. Self-Assembled Fluorescent Bovine Serum Albumin Nanoprobes for Ratiometric pH Measurement inside Living Cells. ACS Appl. Mater. Interfaces. 8, 9629–9634. doi:10.1021/acsami.6b00857

Yannas, I.V., Tobolsky, A.V., 1967. Cross-linking of gelatine by dehydration. Nature, 215, 509-510. DOI: 10.1038/215509b0

Yedomon, B., Fessi, H., Charcosset, C., 2013. Preparation of Bovine Serum Albumin (BSA) nanoparticles by desolvation using a membrane contactor: A new tool for large scale production. Eur. J. Pharm. Biopharm. 85, 398–405. doi:10.1016/j.ejpb.2013.06.014

You, S., Guo, X., Xue, X., Li, Y., Dong, H., Ji, H., Hong, T., Wei, Y., Shi, X., He, B., 2019. PCSK9 Hapten Multicopy Displayed onto Carrier Protein Nanoparticle: An Antiatherosclerosis Vaccine. ACS Biomater. Sci. Eng. 5, 4263-4271. DOI: 10.1021/acsbiomaterials.9b00434

Yu, Z., Yu, M., Zhang, Z., Hong, G., Xiong, Q., 2014. Bovine serum albumin nanoparticles as controlled release carrier for local drug delivery to the inner ear. Nanoscale Res. Lett. 9, 343. DOI: 10.1186/1556-276X-9-343

Zhaparova, L., 2012. Synthesis of nanoparticles and nanocapsules for controlled release of the antitumor drug "Arglabin" and antituberculosis drugs. Eindhoven: Technische Universiteit Eindhoven. doi: 10.6100/IR731636

Zong, S., Pan, F., Zhang, R., Chen, C., Wang, Z., Cui, Y., 2019. Super blinking and biocompatible nanoprobes based on dye doped BSA nanoparticles for super resolution imaging. Nanotechnology. 30, 065701, .DOI: 10.1088/1361-6528/aaf03b

Zwiorek, K., Bourquin, C., Battiany, J., Winter, G., Endres, S., Hartmann, G., Coester, C., 2007. Delivery by Cationic Gelatin Nanoparticles Strongly Increases the Immunostimulatory Effects of CpG Oligonucleotides. Pharm. Res. 25, 551–562. doi:10.1007/s11095-007-9410-5

SUPPORTING INFORMATION

Comparison of methods for measurement of BSA nanoparticle concentration: preliminary study

Bovine serum albumin (BSA, "VWR") was dissolved in water to 50 mg/mL (measured by A_{280}). The pH of aqueous BSA solutions was adjusted to 9 using 1 M NaOH. BSA solution (4 mL) was transferred into a glass vial and heated to +35 °C. With constant stirring on a magnetic stirrer (1400 rpm) 16 mL of 96% ethanol (4 mL/min) was added. The temperature of the solution was monitored using a temperature sensor. Five minutes after the end of the ethanol addition, 640 µl of an 8% aqueous glutaraldehyde solution was added to the suspension. The heating of the suspension was stopped, the cross-linking of nanoparticles was carried out at room temperature for 60 minutes. A suspension of nanoparticles was divided in ~1 mL aliquots, then the nanoparticles were washed from BSA, ethanol, and glutaraldehyde molecules by centrifugation at 20,000 g (1st wash - 30 min, 2nd-4th washes - 10 min). The supernatants after each washing cycle were pooled and stored at +4 °C. After each centrifugation pellets were resuspended using ultrasound (probe diameter 3 mm, amplification 60%, power approximately 8 W, duration 20 sec). After final wash nanoparticles were resuspended in a certain volume of deionized water and stored at +4 °C. Three batches of BSA nanoparticles were prepared (NPA, NPB, and NPC)

Concentration of nanoparticles was measured by direct and indirect Bradford assay, gravimetric analysis (heating at +140 °C), and by alkaline hydrolysis in combination with UV spectroscopy. Results are summarized in tables S1, S2, and S3.

Table S1. Concentrations of nanoparticles prepared during preliminary study determined by different methods (in mg/mL)

Batches	Gravimetric analysis	Bradford, indirect	Bradford, direct	Hydrolysis
NPA	5,56	8,96	1,62	5,24
NPB	6,36	10	1,95	5,88
NPC	7,3	10,97	2,25	6,51

Table S2. Difference of nanoparticle concentrations determined by gravimetric analysis and by various methods (in %). Color scheme reflects the nature of the differences: red - underestimation, green - overestimation

Batches	Gravimetric analysis	Bradford, indirect	Bradford, direct	Hydrolysis
NPA	0,00	61,15	-70,86	-5,76
NPB	0,00	57,23	-69,34	-7,55
NPC	0,00	50,27	-69,18	-10,82

Table S3. Yields of nanoparticles determined by different methods (in % from initial protein concentration)

Batches	Gravimetric analysis	Bradford, indirect	Bradford, direct	Hydrolysis
NPA	47,26	76,16	13,77	44,54
NPB	54,06	85,00	16,58	49,98
NPC	65,70	98,73	20,25	58,59

Table S4. Yields of nanoparticles determined by different methods (in % from initial protein concentration)

Batch	Gravimetric analysis	In relation to BSA concentration measured by UV spectroscopy				In relation to BSA concentration measured by gravimetric analysis				Hydrolysis, In relation to BSA concentration measured by UV spectroscopy	Hydrolysis, In relation to BSA concentration measured by gravimetric analysis
		Bradford assay		BCA assay		Bradford assay		BCA assay			
		Indirect	Direct	Indirect	Direct	Indirect	Direct	Indirect	Direct		
NP1	66,91	66,50	26,80	65,55	27,27	75,74	30,57	74,74	31,10	49,44	56,12
NP2	91,65	83,72	28,03	82,75	37,82	95,43	31,96	94,25	43,08	65,92	74,81
NP3	91,53	82,78	27,46	82,17	33,02	94,51	31,86	93,97	37,76	66,06	74,97
NP4	67,92	73,37	22,46	70,82	33,14	79,98	24,46	77,29	36,10	49,35	56,00
NP5	54,67	70,47	17,20	65,87	23,53	74,67	18,80	71,87	25,60	39,18	44,46
NP6	76,08	71,50	57,89	70,19	74,14	81,57	65,96	80,03	84,49	70,76	80,20
NP7	63,00	58,71	57,23	62,20	65,48	66,75	65,11	70,62	74,48	59,40	67,28
NP8	40,74	ND[1]	ND	ND	ND	ND	ND	38,07	51,45	ND	28,40
NP9	36,95	ND	ND	ND	ND	ND	ND	30,77	52,98	ND	28,03
NP10	74,14	75,52	20,75	76,68	25,54	85,87	36,34	88,84	25,51	52,09	59,12
NP11	76,26	76,80	61,50	72,32	70,65	87,32	69,93	86,07	80,27	73,34	83,26
NP12	60,09	65,10	18,96	67,27	19,69	74,09	22,11	76,31	22,94	ND	ND
NP13	56,61	56,25	23,33	58,39	20,10	63,96	26,67	66,04	23,02	ND	ND

[1] - not done

Table S5. Yields of BSA nanoparticle synthesis reported by different researches

#	Yield	Cross-linking duration	mL of ethanol per mL of BSA/HSA	BSA/HSA conc., mg/mL	pH	Method of BSA/HSA quantification	Ref.
1	39-40%	24 h	4	100 mg/mL	8.2-8.5	Gravimetric analysis (drying for 2 hours at +80 °C)	**Zhaparova, 2012**
2	39%	Overnight	4	62.5 mg/mL	NS[1]	Weighing of lyophilized nanoparticles	**Sozer, 2020**
3	36-94% (depended on ethanol volume)	5 h	4-6 mL	50 mg/mL	9	BCA assay (supernatants)	**Sun, 2018**
4	16-72% (depended on pH and HSA conc.)	24 h	3	10-80 mg/mL	5-9	Gravimetric analysis	**Kimura, 2018**
5	>90%	24 h	4	100 mg/mL	NS	BCA assay (supernatants)	**Weber, 2000**
6	87%	12 h	4	100 mg/mL	8 (in the presence of of 10 mM NaCl)	Gel chromatography	**Wacker, 2011**
7	11%	30 min	2	100 mg/mL	9.4 (in the presence of of 10 mM NaCl)	UV spectrometry (nanoparticle suspension)	**Sánchez-Segura, 2018**
8	72%	30 min	2	100 mg/mL	9.4 (in the presence of of 10 mM NaCl)	NS	**Sánchez-Arreguin, 2019**
9	from 95% at pH 7 to 66% at pH 9	24 h	4	100 mg/mL	7-9 (in the presence of of 10 mM NaCl)	BCA assay (supernatants)	**Langer, 2003**
10	65%-100% (depended on ionic strength)	8 h	4	50 mg/mL	10	BCA assay (supernatants)	**Galisteo-González, 2014**
11	100%	12 h	4	100 mg/mL	8 (in the presence of of 10 mM NaCl)	Gel chromatography	**Von Storp, 2012**
12	approx. 77%	18 h	4	100 mg/mL	9,5 and 10 (in the presence of	Gravimetric analysis	**Kufleitner, 2010**

					of 10 mM NaCl)		

[1] - not specified

Table S6. Difference between actual amount of desolvated protein and amount measured by BCA and Bradford assay

Batch	Actual protein weight, mg	Measured protein weight (BCA assay), mg[1]	% difference BCA assay[2]	Measured protein weight (Bradford assay), mg[1]	% difference Bradford assay[2]
NP1	236,12	ND[3]	-	ND	-
NP2	236,12	99,91	42,31	55,76	23,62
NP3	236,12	88,52	37,49	91,67	38,82
NP4	225,08	120,25	53,43	86,50	38,43
NP5	225,08	117,59	52,24	93,39	41,49
NP6	236,12	247,04	104,62	207,14	87,73
NP7	234,28	201,69	86,09	197,98	84,51
NP8	106,52	Aggregated	-	ND	-
NP9	106,52	Aggregated[4]	-	ND	-
NP10	234,28	89,08	38,02	85,15	36,35
NP11	234,28	198,18	84,59	191,75	81,85
NP12	236,12	114,00	48,28	119,88	50,77
NP13	234,28	121,91	52,04	120,61	51,48

[1] - concentration of BSA calibrators was taken in accordance with gravimetric analysis

[2] - calculated as $mass_{BCA\ (Bradford)}/mass_{actual} x100\%$

[3] - not done

[4] - desolvated gelatin formed a pellet that we couldn't redisperse

Table S7. Turbidity of supernatants after first wash. Measurements were performed in 1 cm cuvette.

Batch	**Absorbance at 600 nm**
NP1	0,153
NP2	0,015
NP3	0,028
NP4	0,06
NP5	0,113

NP6	0,487
NP7	0,477
NP8	0,157
NP9	0,18
NP10	0,028
NP11	0,037
NP12	0,206
NP13	0,127

Table S8. Comparison of BSA calibration curves in BCA assays obtained with two BSA diluents: H_2O vs H_2O + 8% ethanol + 0,025% glutaraldehyde (Fig. S10). Mean absorbances at 562 nm of BSA calibrators were compared by two-way ANOVA with Tukey test. Assays were performed at +37 °C

BSA conc., mg/mL	Difference between mean absorbances	Adjusted P Value
Replication #1		
2	-0,09767	< 0,0001
1	-0,2127	< 0,0001
0,75	-0,182	< 0,0001
0,5	-0,164	< 0,0001
0,25	-0,123	< 0,0001
0,125	-0,061	0,0322
0,0625	-0,04333	0,2276

Replication #2		
2	-0,179	< 0,0001
1	-0,202	< 0,0001
0,75	-0,173	< 0,0001
0,5	-0,1403	< 0,0001
0,25	-0,08567	0,0007
0,125	-0,049	0,1257
0,0625	-0,02433	0,7542
Replication #3		
2	-0,336	< 0,0001
1	-0,2773	< 0,0001
0,75	-0,2517	< 0,0001
0,5	-0,221	< 0,0001
0,25	-0,1807	< 0,0001
0,125	-0,1453	< 0,0001
0,0625	-0,09167	0,009

Table S9. Comparison of BSA calibration curves in Bradford assays obtained with two BSA diluents: H_2O vs H_2O + 8% ethanol + 0,025% glutaraldehyde (Fig. S11). Mean absorbances at 595 nm of BSA calibrators were compared by two-way ANOVA with Tukey test.

BSA conc., mg/mL	Difference between mean absorbances	Adjusted P Value
Replication #1		

2	-0,07267	0,1336
1	-0,05733	0,3397
0,75	-0,056	0,3635
0,5	-0,03733	0,7389
0,25	-0,023	0,943
0,125	-0,02367	0,9371
0,0625	-0,01933	0,9692
Replication #2		
2	-0,03067	0,5658
1	0	> 0,9999
0,75	-0,02	0,864
0,5	-0,01567	0,9393
0,25	-0,02967	0,597
0,125	-0,02967	0,597
0,0625	-0,02567	0,7188
Replication #3		
2	-0,01733	0,9716
1	0,03867	0,6421
0,75	-0,03	0,8207
0,5	-0,008667	0,998

0,25	-0,009333	0,9973
0,125	-0,009333	0,9973
0,0625	-0,013	0,9903

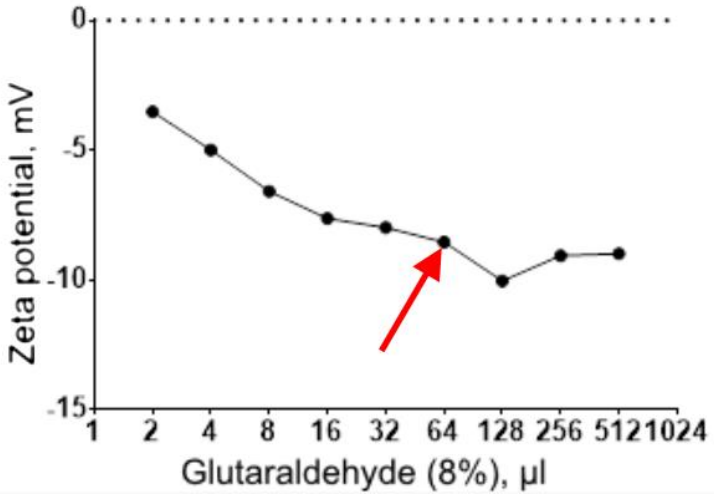

Fig. S1. Effect of glutaraldehyde volume on zeta potential of desolvated nanoparticles. 4 mL of 50 mg/mL BSA was desolvated with 16 mL of 96% ethanol. Resulting mixture was divided into 10 vials (400 µl of 50 mg/mL per vial). Certain volume of glutaraldehyde (8%) was added to each vial. Zeta potential was measured without washing. Chosen glutaraldehyde volume is marked with an arrow.

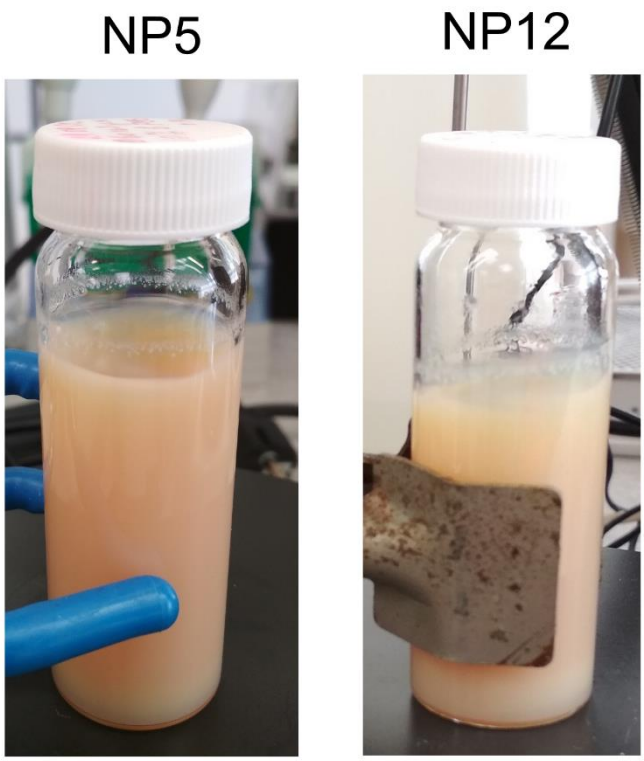

Fig. S2. Different degree of protein sedimentation on the walls of vial in the course of cross-linking

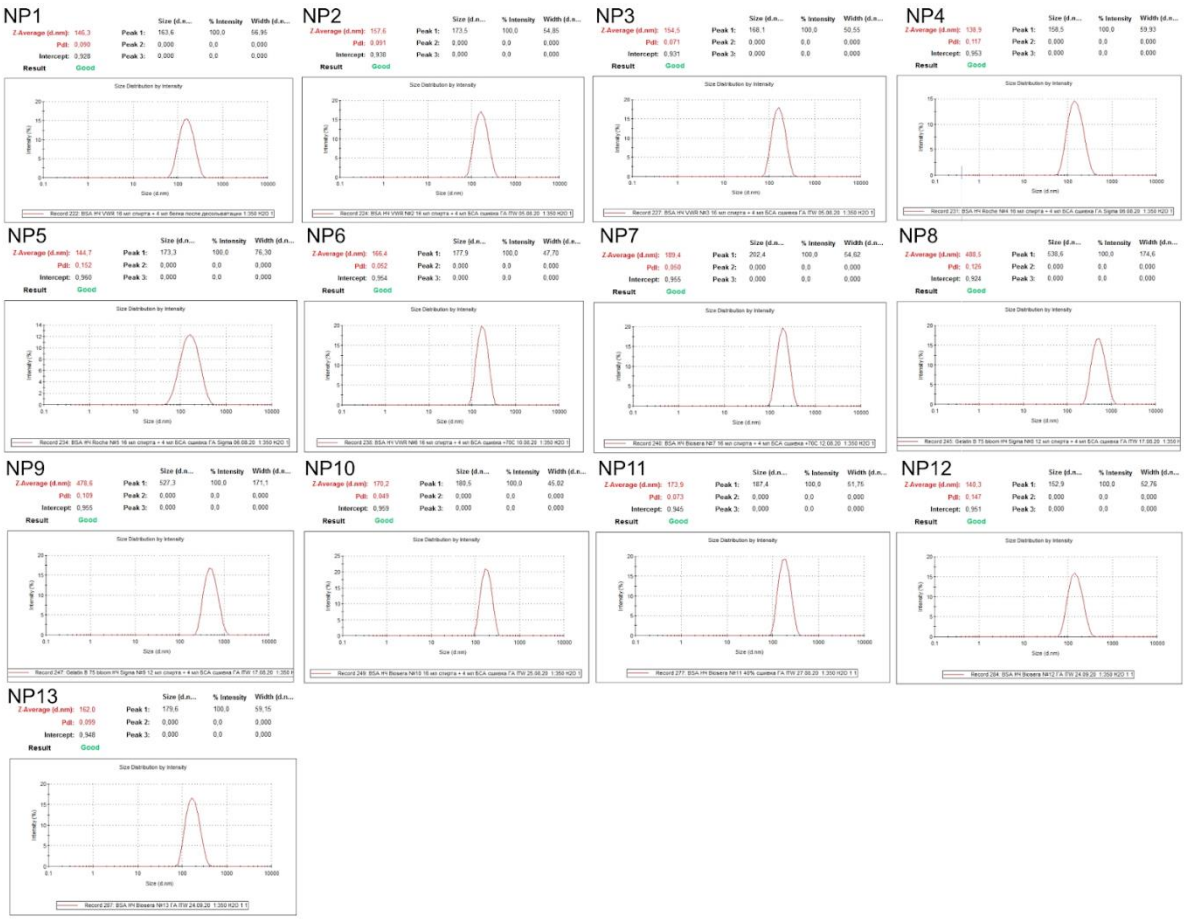

Fig. S3. Intensity-weighted size distributions o NP1-NP13

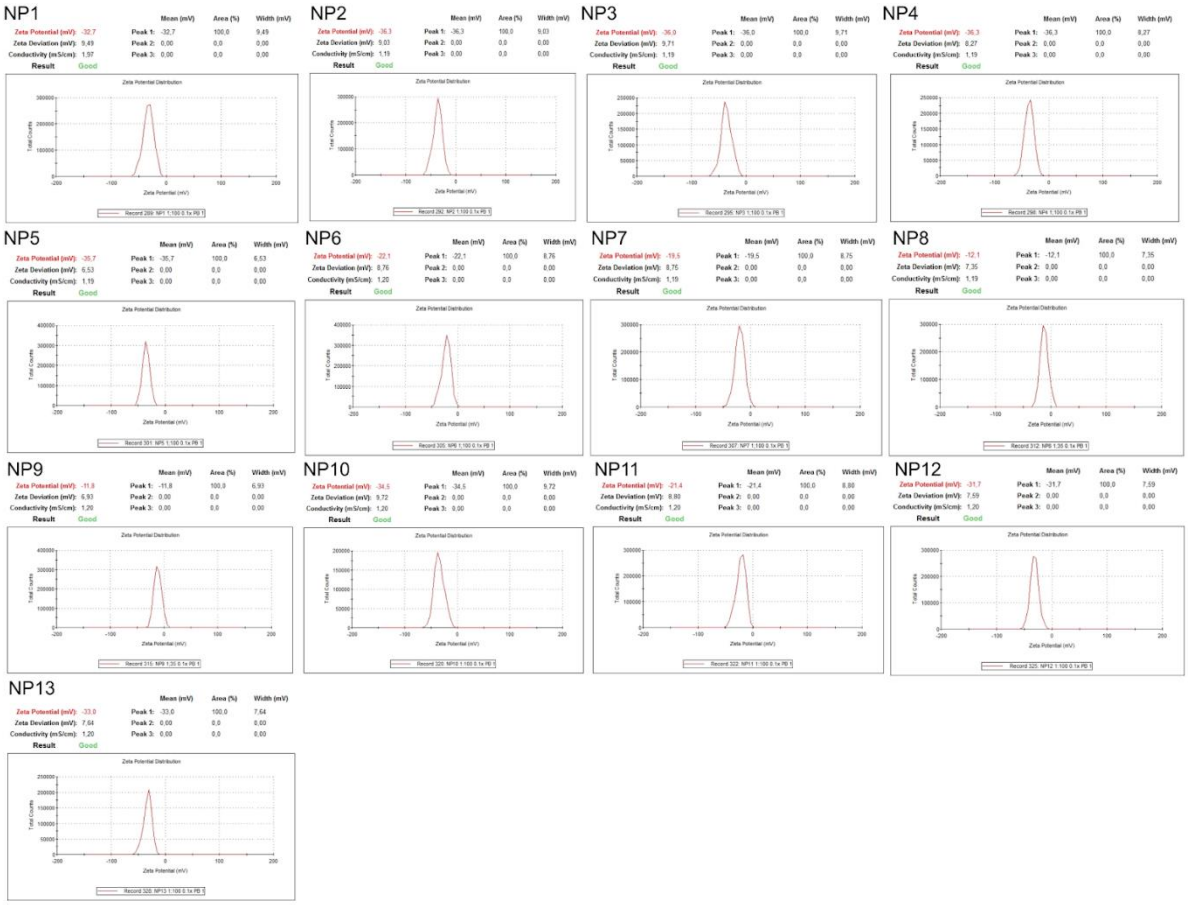

Fig. S4. Zeta-potential distributions o NP1-NP13

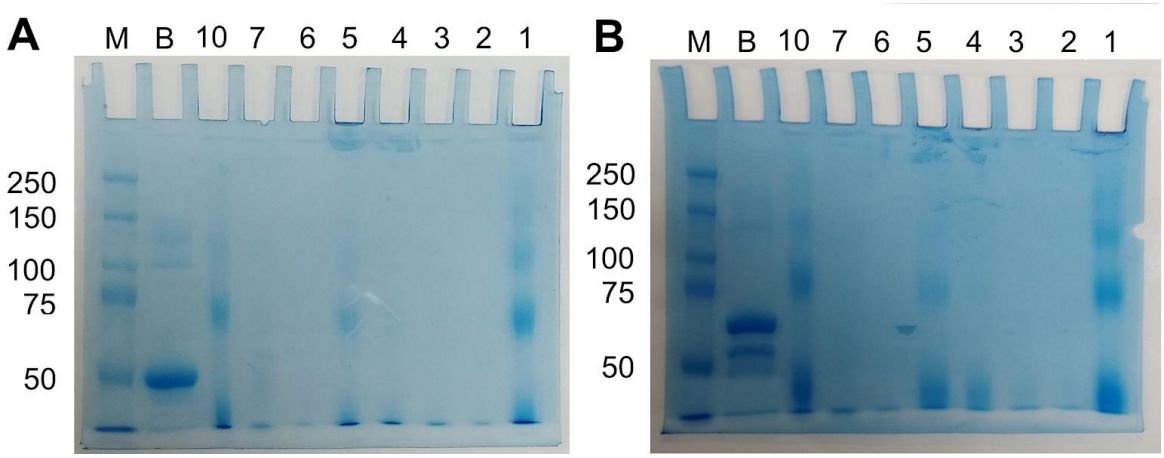

Fig. S5. A - SDS-PAGE of 1st wash supernatants of NP1-NP7 and NP10 in non-reducing conditions. B - SDS-PAGE of 1st wash supernatants of NP1-NP7 and NP10 in reducing conditions. Legend: B - BSA. M - protein markers. Concentrations: BSA - 1 mg/mL, nanoparticles - 1 mg/mL (as determined by gravimetric analysis). Polyacrylamide concentration is 6%, voltage - 200 mV.

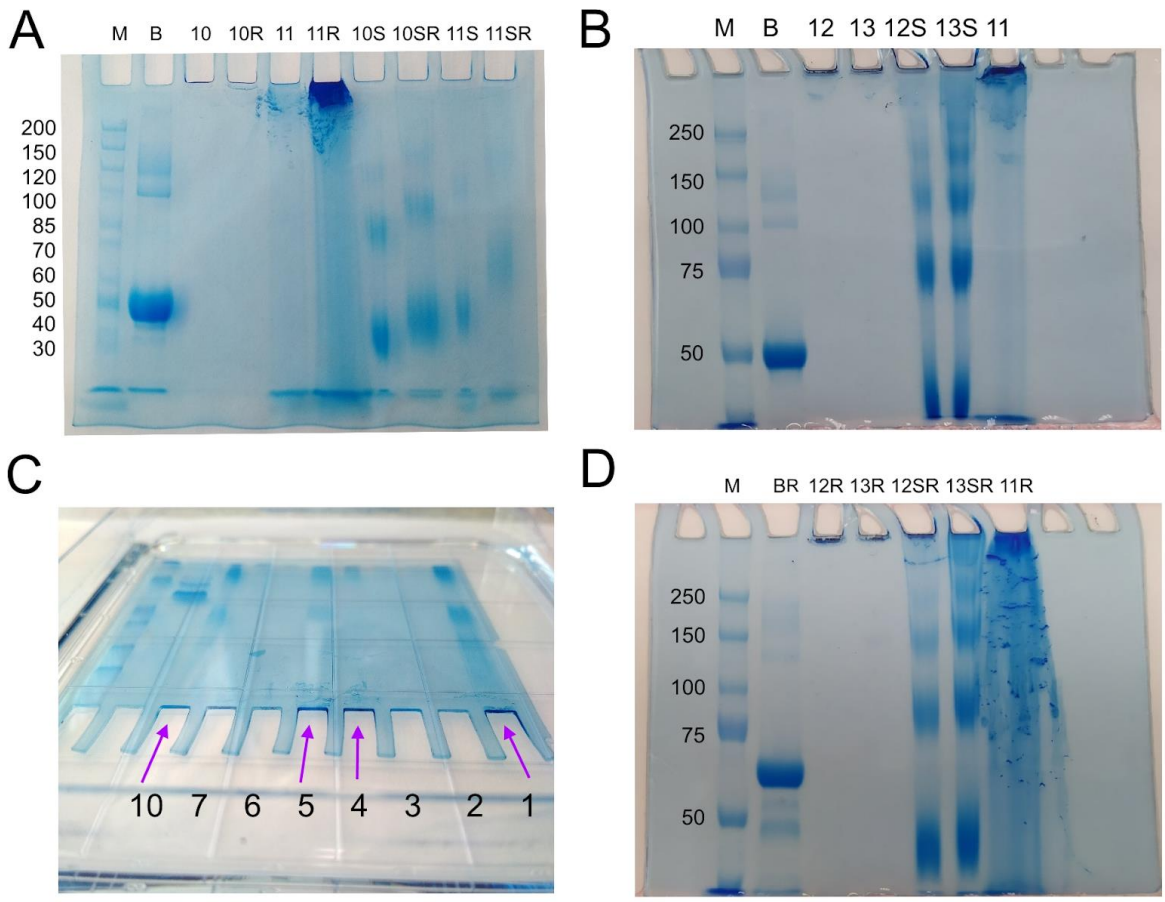

Fig. S6. A, B, D - SDS-PAGE of NP10-13 and 1st wash supernatants (S) of NP10-13 in reducing (R) and non-reducing conditions. NP11 were analyzed twice: in 1 (A) and 6 (B,D) weeks after the preparation. C - nanoparticles at the bottom of the gel wells (gel from fig. SI5B). Legend: B - BSA. M - protein markers. Concentrations: BSA - 1 mg/mL, nanoparticles - 1 mg/mL (as determined by gravimetric analysis). Polyacrylamide concentration is 6%, voltage - 200 mV.

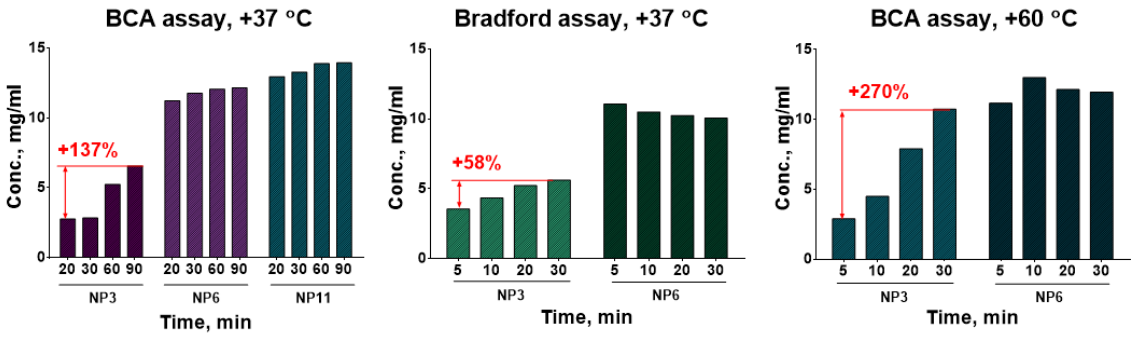

Fig. S7. Dependence of measured concentration upon incubation time and temperature for protein nanoparticles with different cross-linking type.

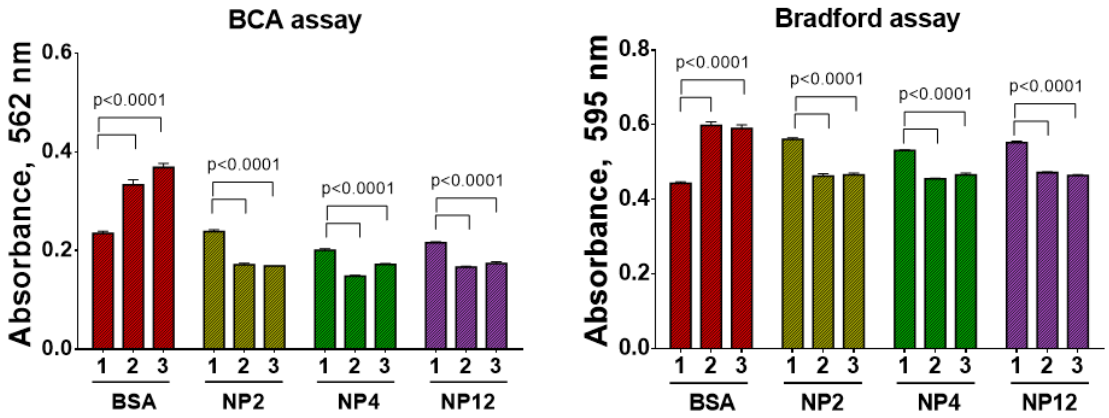

Fig. S8. BCA assay and Bradford assay of BSA (14 mg/mL) and BSA nanoparticles (undiluted) mixed with NaOH (final concentration 4 M) and incubated for 48 h at +37 °C (1); kept at +37 °C for 48 h and mixed with NaOH (final concentration 4 M) prior to assay (2); mixed with water and incubated for 48 h at +37 °C. Volume of all samples was equal. All samples were diluted 1:40 with water before measurement. Mean absorbances were compared by two-way ANOVA with Tukey test. n=3, mean±SD.

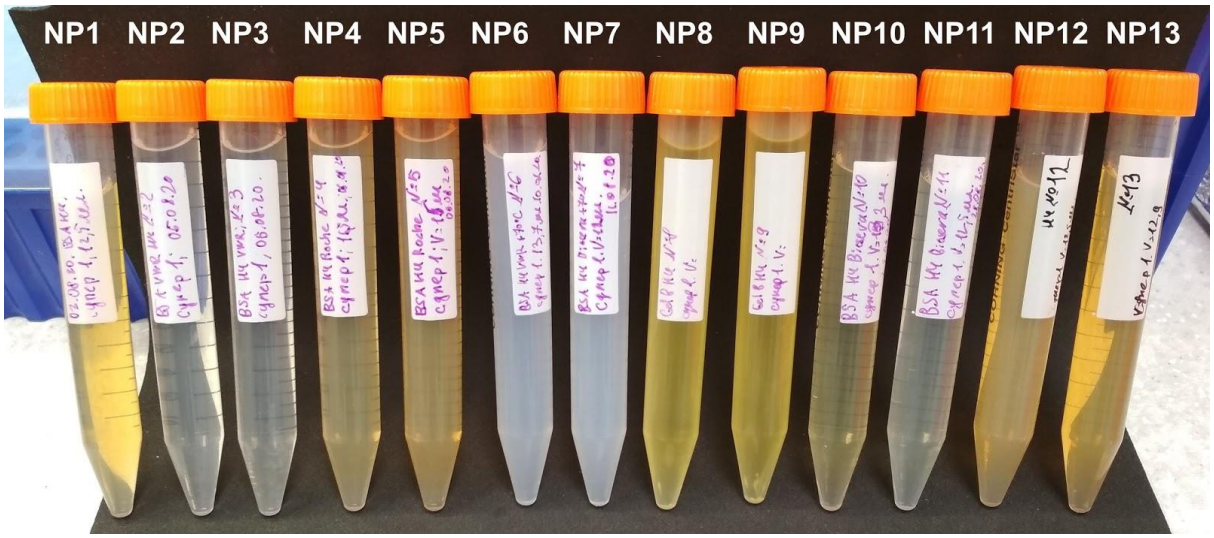

Fig. S9. Supernatants after the first wash of nanoparticles

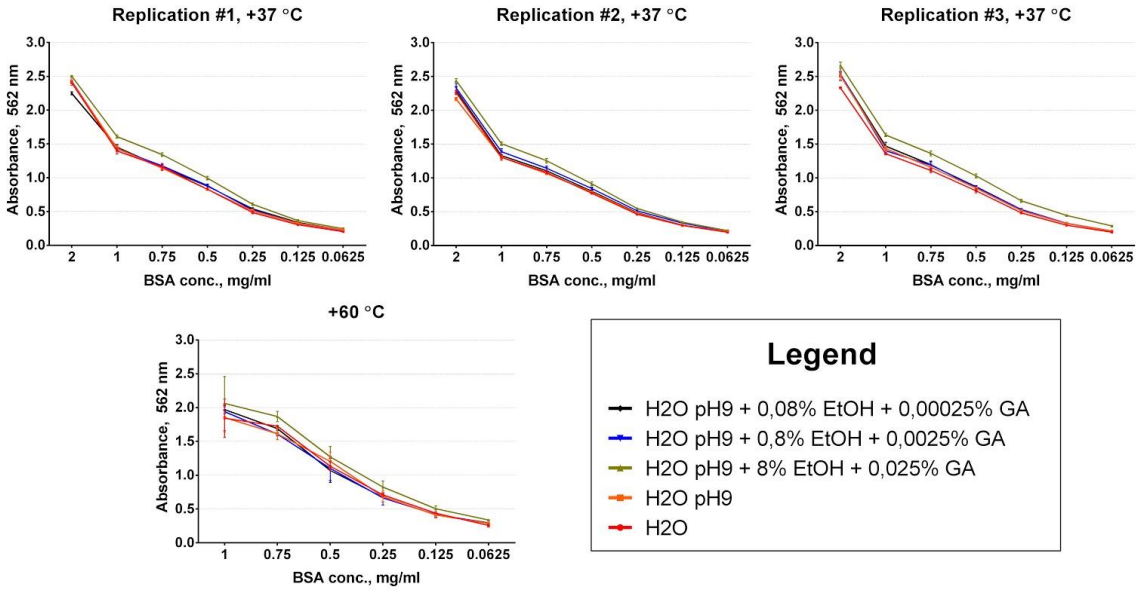

Fig. S10. Influence of ethanol (EtOH) and glutaraldehyde (GA) on the BCA assay of BSA. All experiments were performed on different days. Incubation was carried out at +37 °C for 30 min or at +60 °C for 15 min.

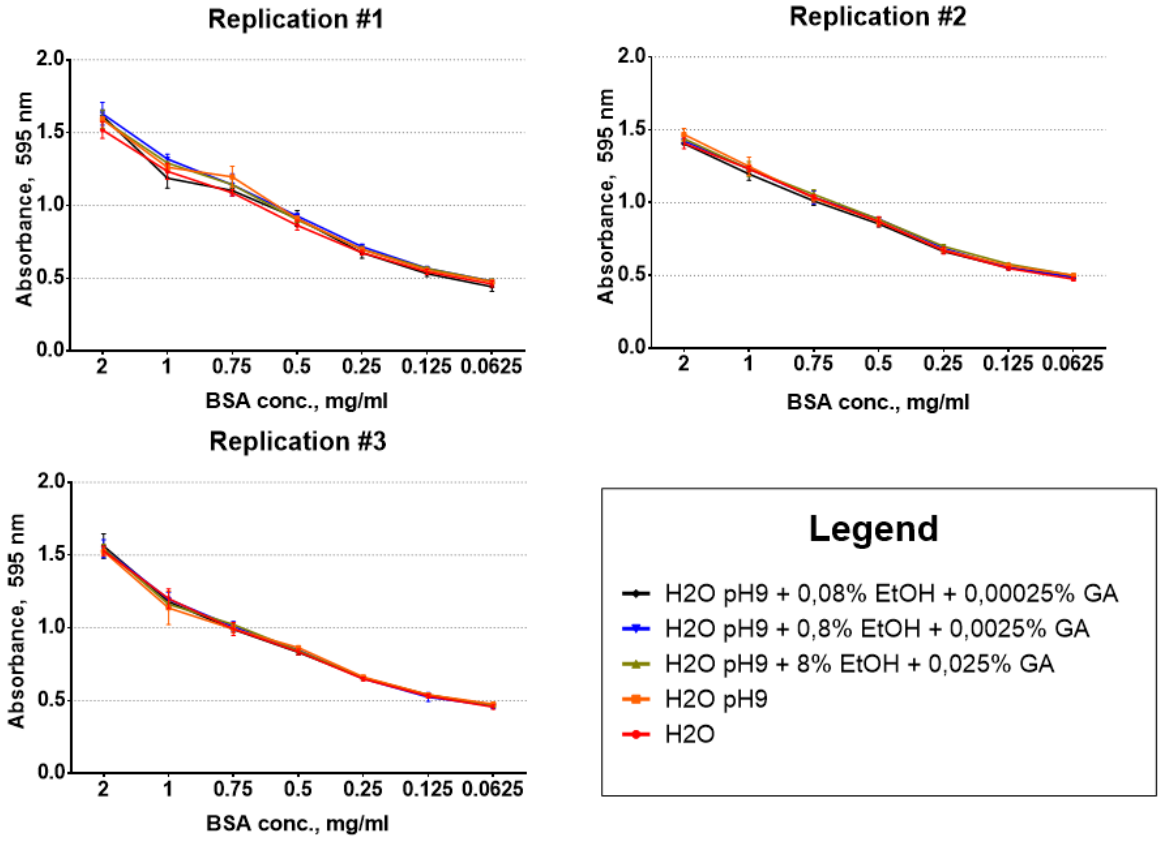

Fig. S11. Influence of ethanol (EtOH) and glutaraldehyde (GA) on the Bradford assay of BSA. Three experiments were performed on different days.

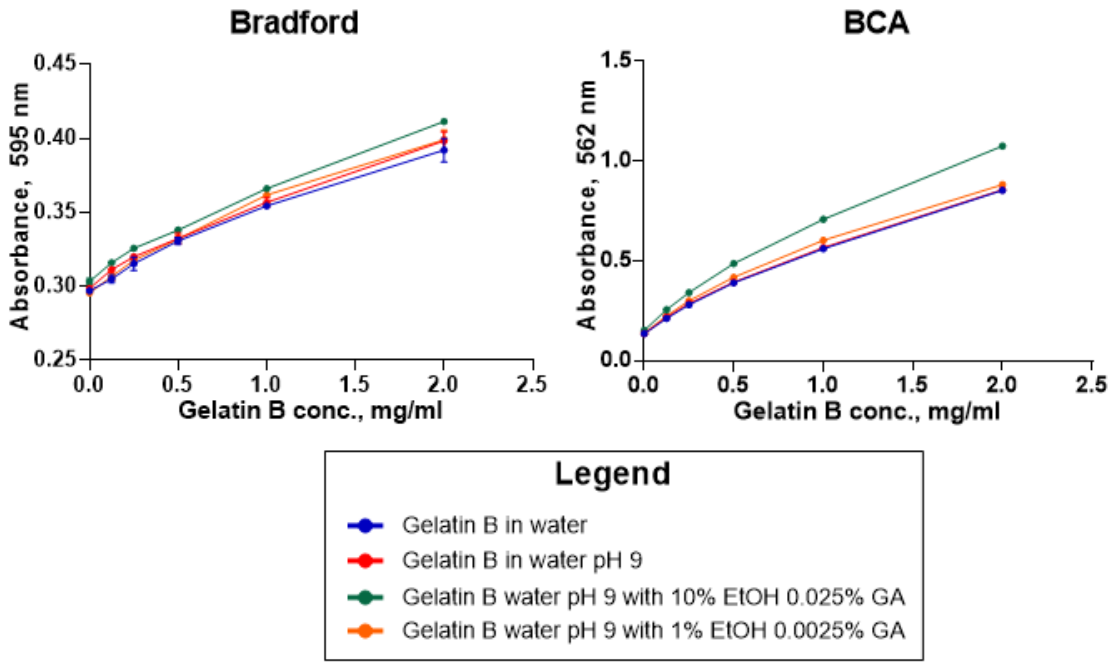

Fig. S12. Calibration curves of gelatin B in BCA and Bradford assays in the presence of different amounts of ethanol and glutaraldehyde. EtOH - ethanol, GA - glutaraldehyde

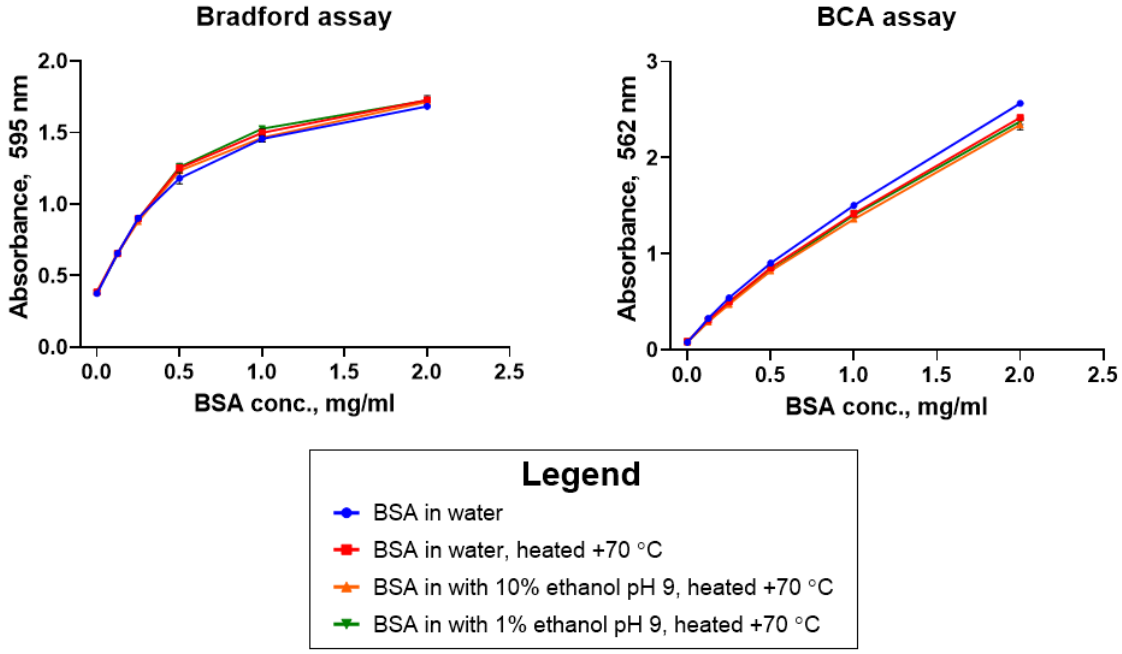

Fig. S13. Influence of BSA heating on the BCA and Bradford assays.

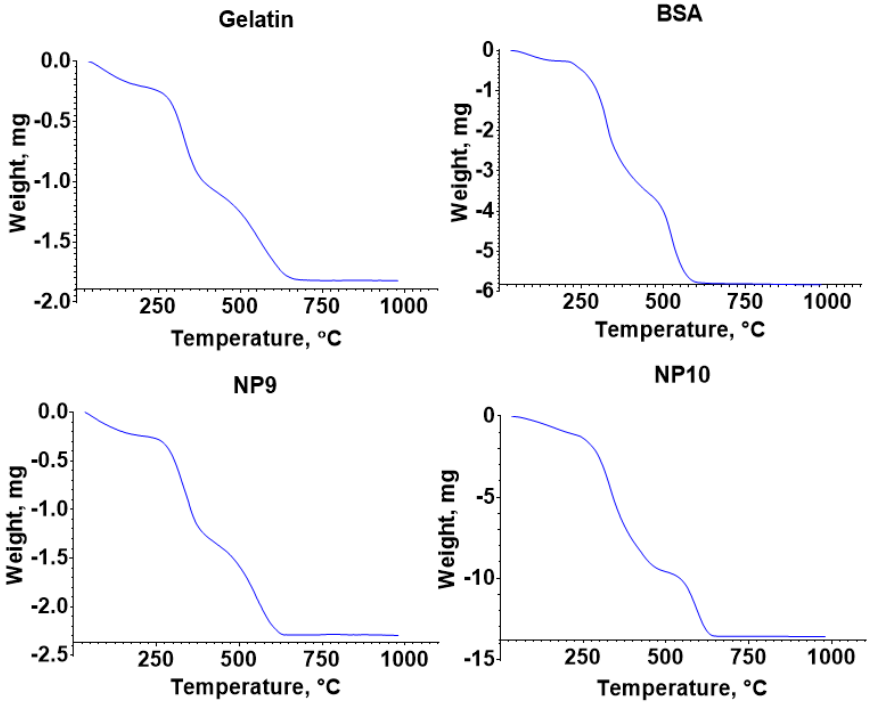

Fig. S14. TGA curves of BSA, gelatin B and corresponding nanoparticles

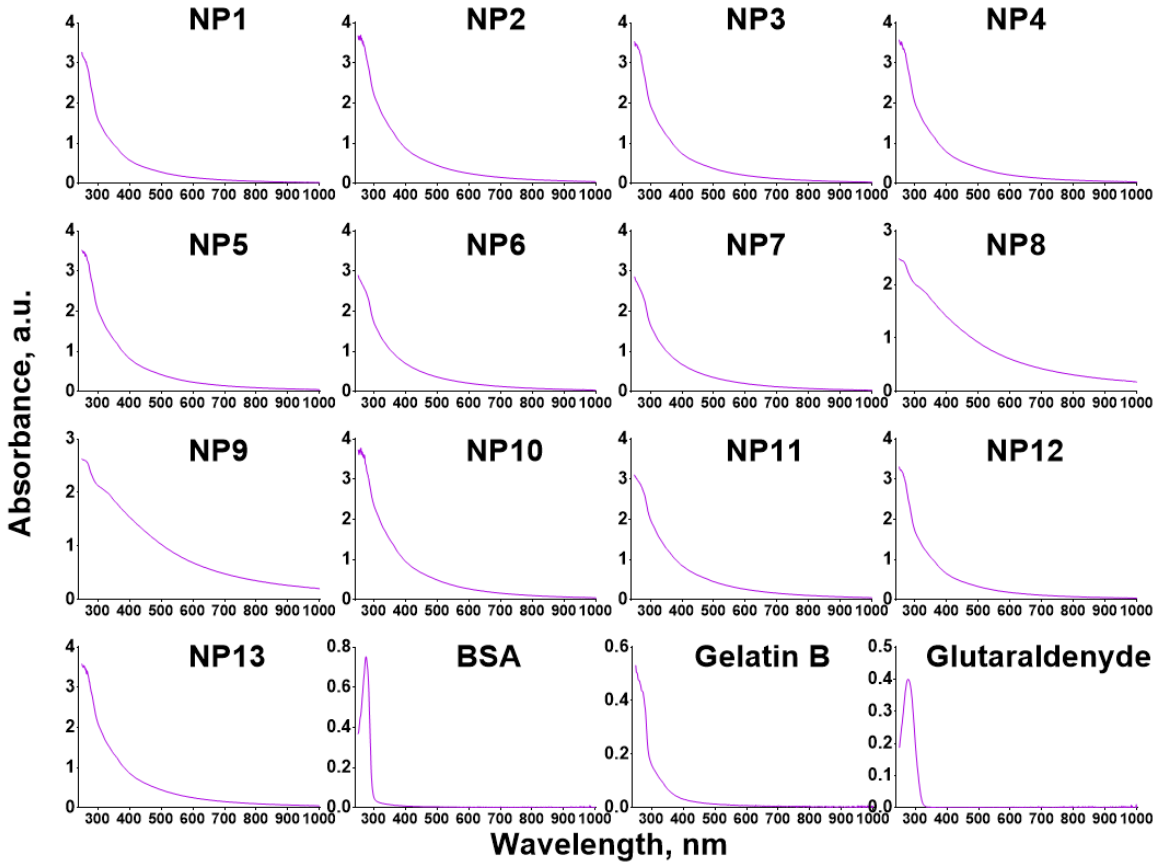

Fig. S15. UV-vis spectra of BSA and gelatin nanoparticles, BSA, gelatin and glutaraldehyde. Concentrations: nanoparticles - 1 mg/mL (by gravimetry), BSA - 1 mg/mL (by gravimetry), gelatin B - 5 mg/mL, glutaraldehyde - 0,5%.

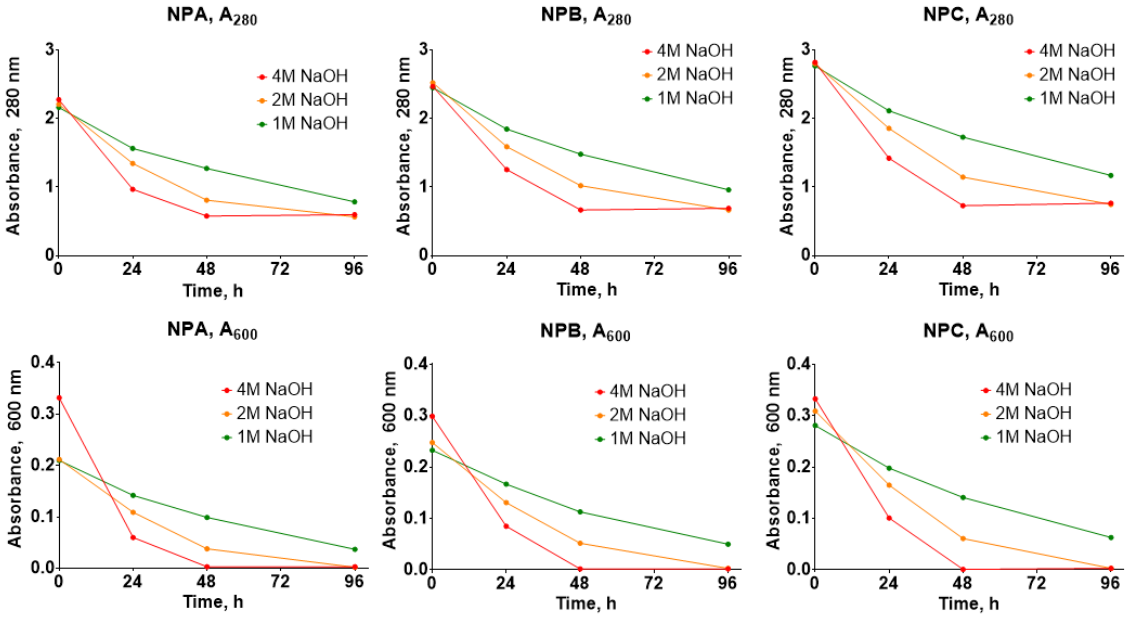

Fig. S16. Optimization of hydrolysis conditions during preliminary studies. Change of nanoparticle absorbance at 280 and 600 nm after the incubation with different concentrations of NaOH. 10 M NaOH was added to 1 mL of undiluted nanoparticles, volume was adjusted to 1666 µL with water. Hydrolyzates were diluted 1:10 with water before measurement of absorbance. NPA, NPB, NPC - batches of BSA nanoparticles synthesized in preliminary experiments (see tables S1, S2, and S3)

References (SI)

Galisteo-González, F., Molina-Bolívar, J. A., 2014. Systematic study on the preparation of BSA nanoparticles. Colloid. Surface B. 123, 286–292. doi:10.1016/j.colsurfb.2014.09.028

Kimura, K., Yamasaki, K., Nakamura, H., Haratake, M., Taguchi, K., Otagiri, M., 2018. Preparation and in vitro analysis of human serum albumin nanoparticles loaded with anthracycline derivatives. Chem. Pharm. Bull. 66, 382-390. DOI: 10.1248/cpb.c17-00838

Kufleitner, J., Worek, F., Kreuter, J., 2010. Incorporation of obidoxime into human serum albumin nanoparticles: optimisation of preparation parameters for the development of a stable formulation. J. Microencapsul. 27, 594–601. doi:10.3109/02652048.2010.501395

Langer, K., Balthasar, S., Vogel, V., Dinauer, N., Von Briesen, H., Schubert, D., 2003. Optimization of the preparation process for human serum albumin (HSA) nanoparticles. Int. J. Pharm. 257, 169-180. DOI: 10.1016/S0378-5173(03)00134-0

Sánchez-Arreguin, A. Carriles, R. Ochoa-Alejo, N. López, M.G. Sánchez-Segura, L., 2019. Generation of BSA-capsaicin Nanoparticles and Their Hormesis Effect on the Rhodotorula mucilaginosa Yeast. Molecules. 24, 2800.

Sánchez-Segura, L., Ochoa-Alejo, N., Carriles, R., Zavala-García, L. E., 2018. Development of bovine serum albumin–capsaicin nanoparticles for biotechnological applications. Appl. Nanosci. 8, 1877–1886. doi:10.1007/s13204-018-0874-x

Sozer, S. C., Egesoy, T. O., Basol, M., Cakan-Akdogan, G., Akdogan, Y., 2020. A simple desolvation method for production of cationic albumin nanoparticles with improved drug loading and cell uptake. J. Drug Deliv. Sci. Technol. 101931. doi:10.1016/j.jddst.2020.101931

Sun, S., Xiao, Q.-R., Wang, Y., Jiang, Y., 2018. Roles of alcohol desolvating agents on the size control of bovine serum albumin nanoparticles in drug delivery system. J. Drug Deliv. Sci. Technol. 47, 193–199. doi:10.1016/j.jddst.2018.07.018

Von Storp, B., Engel, A., Boeker, A., Ploeger, M., Langer, K., 2012. Albumin nanoparticles with predictable size by desolvation procedure. J. Microencapsul. 29, 138–146. doi:10.3109/02652048.2011.635218

Wacker, M., Zensi, A., Kufleitner, J., Ruff, A., Schütz, J., Stockburger, T., Marstaller, T., Vogel, V., 2011. A toolbox for the upscaling of ethanolic human serum albumin (HSA) desolvation. Int. J. Pharm. 414, 225–232. doi:10.1016/j.ijpharm.2011.04.046

Weber, C., Coester, C., Kreuter, J., Langer, K., 2000. Desolvation process and surface characterisation of protein nanoparticles. Int. J. Pharm. 194, 91–102. doi:10.1016/s0378-5173(99)00370-1

Zhaparova, L., 2012. Synthesis of nanoparticles and nanocapsules for controlled release of the antitumor drug "Arglabin" and antituberculosis drugs. Eindhoven: Technische Universiteit Eindhoven. doi: 10.6100/IR731636